Portland Cement Concrete Pavement Thickness Variation Versus Observed Pavement Distress

Lev Khazanovich, Principal Investigator
Department of Civil, Environmental, and Geo- Engineering
University of Minnesota

September 2016

Research Project
Final Report 2016-30

Minnesota Department of Transportation

RESEARCH SERVICES & LIBRARY

Office of Transportation System Management

To request this document in an alternative format, such as braille or large print, call 651-366-4718 or 1-800-657-3774 (Greater Minnesota) or email your request to ADArequest.dot@state.mn.us. Please request at least one week in advance.

Technical Report Documentation Page

1. Report No.	2.	3. Recipients Accession No.
MN/RC 2016-30		

4. Title and Subtitle	5. Report Date
Portland Cement Concrete Pavement Thickness Variation Versus Observed Pavement Distress	September 2016
	6.

7. Author(s)	8. Performing Organization Report No.
Lev Khazanovich, Kyle Hoegh, Randal Barnes, Ryan Conway, Lucio Salles	

9. Performing Organization Name and Address	10. Project/Task/Work Unit No.
Department of Civil, Environmental, and Geo- Engineering University of Minnesota 500 Pillsbury Drive SE Minneapolis, MN 55455	CTS #2015024
	11. Contract (C) or Grant (G) No. (c) 99008 (wo) 156

12. Sponsoring Organization Name and Address	13. Type of Report and Period Covered
Minnesota Department of Transportation Research Services and Library 395 John Ireland Blvd., MS 330 St. Paul, MN 55155	Final Report
	14. Sponsoring Agency Code

15. Supplementary Notes
http://www.mndot.gov/research/reports/2016/201630.pdf

16. Abstract (Limit: 250 words)

Benefits from a potential significant correlation between distresses and slab thickness can be broadly applied in all stages of highway development from design and construction to maintenance decisions. In order to comprehensive explore this possibility, thickness data and existing distresses were related for three highway projects in Minnesota. Thickness was obtained through non-destructive ultrasonic testing, while distresses were recorded for the same location with a distress image software. Significant thickness variation was observed in both longitudinal and transverse directions. The combined results of thickness, shear wave velocity and distresses analysis revealed that an increase in shear wave velocity was coincident with a less damaged pavement area within a section. An in-depth statistical analysis confirmed this observation showing that shear surface velocity variation was better correlated with overall pavement performance than thickness variation. Differences in cracking behavior within a section were traced back to changes in construction and design practices, showing the potential of using shear velocity analysis for pavement maintenance. A survey and analysis procedure for shear wave velocity testing of concrete pavements is proposed.

17. Document Analysis/Descriptors	18. Availability Statement
nondestructive tests, thickness, pavement distress, rigid pavements, concrete pavements, ultrasonic tests, tomography	No restrictions. Document available from: National Technical Information Services, Alexandria, Virginia 22312

19. Security Class (this report)	20. Security Class (this page)	21. No. of Pages	22. Price
Unclassified	Unclassified	50	

Portland Cement Concrete Pavement Thickness Variation Versus Observed Pavement Distress

Final Report

Prepared by

Lev Khazanovich
Randal Barnes
Ryan Conway
Lucio Salles
Department of Civil, Environmental, and Geo- Engineering
University of Minnesota

Kyle Hoegh
Office of Materials and Road Research
Minnesota Department of Transportation

September 2016

Published by

Minnesota Department of Transportation
Research Services & Library
395 John Ireland Boulevard, MS 330
St. Paul, Minnesota 55155-1899

TABLE OF CONTENTS

LIST OF FIGURES

LIST OF TABLES

Executive Summary

Concrete slab thickness is the key characteristic of a concrete pavement. It is the most important design parameter and the major focus of control and inspection during construction. Most road agencies, including the Minnesota Department of Transportation (MnDOT), have adopted contractor compensation adjustments based on the thickness of constructed pavements. Although it is commonly believed that an excess in concrete thickness increases pavement longevity, there is only anecdotal evidence to support this claim.

The major reason for the lack of data on the relationship between concrete pavement thickness parameters and pavement performance results from the destructive nature of thickness measurements. Concrete thickness is typically assessed by coring: a destructive, expensive and time-consuming that which offers only widely spaced measurements of thickness. However, recent advances in the nondestructive testing of pavements, such as the use of ultrasonic shear-wave tomography devices, allow for large-scale, rapid collection of reliable pavement thickness measurements. In addition to thickness, ultrasonic tomography is also capable of in-situ determination of shear wave velocity (SWV) at the slab surface, an important indicator of material properties that can be related to material strength.

The research described in this report has the main goal of investigating a potential correlation between distress occurrence and thickness or SWV variation. Thickness/SWV data were obtained using ultrasonic shear-wave tomography devices commonly referred to as “MIRA” devices. MIRA was applied to test sites, while surface distresses at those sites were visually recorded.

Four distress surveys were conducted using MIRA on three roadways in Minnesota. Single surveys were conducted on both Highway 100 and Interstate 394, and two surveys were conducted on Highway 60. Over eight-thousand measurements were collected along with continuous distress surveys. A dense survey pattern consisting of 10 transverse measurements taken every 10 feet produced detailed data which provided insight into small scale thickness and SWV variability. The distress survey was conducted in accordance with MnDOT protocol, with modifications allowing for precise location recording of observed distress. Observed distress was then associated with MIRA measurements within 5 feet longitudinally for comparative analysis.

The findings of the MIRA surveys show that both pavement thickness and SWV are highly variable both in the longitudinal and transverse directions. The scale of the variations was found to be similar in both the transverse and longitudinal directions, with approximately a 0.5-inch of variation per 10 feet. Interestingly, three of the four surveys conducted reported average thickness less than design thickness, a result contrary to what is typically reported. Similar to thickness, SWV data was found to have similar variability in the transverse and longitudinal directions. Interestingly, locations where construction changes occurred were easily identifiable in the SWV data in two of the four surveys. Distress surveys showed that the roadways studied had different distress profiles. In some roadways, distress was dominated by spalling and little cracking was observed. In other surveys, cracking was the dominant distress.

Both visual and logistic regression analysis suggest that exceeding the design thickness does not correlate to increased pavement performance. Investigation of plots of pavement thickness show high distress concentrations in regions that are thickness deficient as well as in regions where design thickness was exceeded. Additionally, statistical analysis did not show a relationship between excess thickness and decreasing distress occurrence. However, in two of the four surveys conducted (both on Highway 60), the transverse slope in thickness was found to be significantly correlated with observed distress. Specifically, it was found that slabs that had a decrease in thickness from left to right (in the direction of traffic), exhibited higher rates of cracked and broken panels than slabs that did not. However, this trend was not observed in the other roadways surveyed. Visual and statistical analysis of SWV data showed more promising correlations. Investigation of the plots of SWV and observed distress shows that a drop in SWV corresponded to an increase in distress occurrence. This was particularly true for both Highway 60 surveys, where a change in construction was surveyed. The change in construction produced a large drop in SWV and large increase in the rate of distress occurrence. Logistic regression analysis of the other datasets taken on I 394 and Highway 100 also produced highly significant correlations between distress occurrence and decreasing SWV.

While the results discussed here are limited by the small number of analyzed sections, they illustrate the importance of material quality and uniformity of control during construction, since alterations in material properties (SWV) may significantly influence pavement performance. The inconclusive thickness results should not be taken to imply pavement thickness is irrelevant to performance, or that contractors should not be penalized for thickness deficiencies, as the pavement still needs to have sufficient thickness to carry its intended traffic loadings over its service life. Additionally, the application of MIRA presented in this report shows that an ultrasonic SWV survey is an appropriate test to identify changes in construction and design that could lead to higher rates of distress occurrence.

CHAPTER 1: INTRODUCTION

Slab thickness is the key design aspect of concrete pavements. It is the most important output of design models and the major focus of control and inspection during and after construction. Basic pavement knowledge suggests that an excess in constructed thickness implies in economic loss while thickness deficiencies can reduce pavement performance. This basic assumption has lead most road agencies, including the Minnesota Department of Transportation (MnDOT) to adopt contractor compensation deductions for thickness deficiencies (MnDOT, 2005). Consequently, contractors have a tendency of building slabs slightly thicker than the design procedure recommends (Stubstad et al, 2002; Jiang, et al, 2003; Kim and McCullough, 2002). Though contractor practices typically result in thicker pavements, actual field correlation between surface and subsurface pavement distress and excessive slab thickness has not been conclusive.

The lack in field validation of the performance-thickness relationship results from the destructive nature of thickness determination via coring, which is time consuming and expensive. Additionally, the process of coring often creates surface or subsurface damage. These drawbacks make complete and thorough thickness validation unrealistic and result in measurements which are widely spaced and generally only taken in the middle of the slab. For example, MnDOT QA/QC calls for exploratory cores to be drilled initially every 1000 ft and at smaller spacing only if a deficiency is encountered. These coring practices result in widely spaced longitudinal data which gives little insight to the small scale longitudinal thickness variation and no information about transverse thickness variation and their potential impacts on performance. Recent advances in nondestructive testing allow for a much more thorough characterization of pavement quality. In particular, the MIRA ultrasonic tomographer allows for large scale, rapid collection of closely spaced measurements of pavement thickness. Use of the MIRA has shown the particular ability to very precisely and accurately determine PCC layer thickness (Hoegh, et al., 2010; Vancura, 2013; Edwards, 2012). Moreover, unlike field distress surveys which only include observed surface distress, MIRA has shown promise in identifying surface and internal distress (Freeseman et al., 2016a), both visible and incipient.

Vancura (2013) conducted a large scale study on MIRA results and coring. Statistical analysis showed that MIRA measurements were able to predict the average thickness determined by coring. Additionally, MIRA measurements were better able to find maximum and minimum thickness values. Another interesting finding was that pavement showed large degrees of variation in the traverse direction and that pavement tended to be thicker in the middle and thinner near the edge. In some locations this discrepancy was as high as 38 mm (1.5 in.).

Though thickness is the key structural design parameter in pavements, MIRA is also capable of in-situ determination of shear wave velocity (SWV) at the slab surface, an important indicator of material properties. MIRA allows shear wave velocity computation from analysis of the direct (un-reflected) first arrival of shear waves. Shear wave velocity is a function of Young's modulus, Poisson's ratio, and pavement density (Heisey, et al., 1982) and can be used to compute compressive strength (An, et al., 2009). Multiple studies have found strong correlations between compressive strength and shear wave velocity (Freeseman, et al. 2016b; Cho, et al., 2007; An, et al, 2009). Though lab studies have been performed, large scale field studies of pavement shear

wave velocity variation, or using pavement shear wave velocity as an indicator of pavement quality, have not yet been conducted. Also, some state and federal transportation agencies have explored pavement shear wave velocity as measure of pavement quality but implementation has been limited.

The research described in this report has the main goal of investigating a potential correlation between concrete pavement distresses with thickness or shear surface velocity variation. Thickness/shear wave velocity data was obtained through ultrasonic measurements, while surface distresses were recorded and analyzed by an imaging software currently in use by the MnDOT. Construction records were reviewed to investigate different results. Additionally, an in-depth statistical analysis was performed in order to investigate possible thickness/distress or velocity/distress relations using several predictors.

CHAPTER 2: DATA COLLECTION AND PROCESSING

This chapter describes data acquisition and processing. Data collection was performed in two lines of surveys: ultrasonic measurements for thickness and distress surveys using distress image software and visual observation. Data processing was done to obtain thickness and shear wave velocity data from the ultrasonic testing and to combine this output with the distress results.

2.1 Highway Projects Selected

Pavement thickness and distress data were collected at three locations within Minnesota. These locations included Minnesota State Highway 60 (Highway 60), Minnesota State Highway 100 (Highway 100) and Interstate 394 (I-394). All surveys were performed in the driving lane (truck lane), with the exception of I-394, which was performed in a center corridor. Surveys performed on Highway 60 were taken in east and west directions. All pavements surveyed were jointed reinforced concrete pavement (JRCP). A visual distress survey of each investigated section was conducted to verify the distress survey that was performed using the Pathview II software. The visual distress and the MIRA measurements surveys produced six datasets of spatially related data, including pavement thickness, shear wave velocity, and distress. The design data of the investigated sections was compiled by MnDOT and is presented in Table 1 [1]. General details of the surveys are described below.

- Minnesota State Highway 60 (Highway 60): The survey of Highway 60 was performed on the 9th of June, 2015. A survey was performed in both the eastbound and westbound direction of this 4-lane divide highway. The east survey extended 1990 ft. located approximately from MP52+5227 ft. to MP53+1954 ft. The west survey was performed in reverse direction ranging over 2990ft with an end point at MP52+4224 ft. As can be seen in Table 1, the east and west portions of Highway 60 were constructed in different years. A total of 2000 and 3000 MIRA measurements were performed for the east and west portions, respectively.

- Minnesota State Highway 100 (Highway 100): The survey of Highway 100 (North) was performed on the 31st of May, 2015. The 1620ft investigation section ranged from approximately MP3+ 4380ft to MP4+620ft. A total of 1630 MIRA measurements were performed.

- Interstate 394 (I-394): The survey of I-394 was performed on the 9th of July, 2015. The 1990ft investigation sections was located approximately from MP6+4285ft. to MP7+995ft. A total of 2000 MIRA measurements were collected.

Table 1 - Design data for the selected sections

Section	Beginning - Ending MP	PCC Design Thick. mm (in.)	Date Completed	Base Layer Material	Base Thick. mm (in.)	Drainage
Highway 100	3.39 - 4.64	228.6 (9)	10/1/1973	Crushed Gravel	330.2 (13)	Long. Drains
Highway 60 (1)	49.91 – 53.27	203.2 (8)	10/1/1988	Crushed Gravel	127 (5)	Long. Drains
Highway 60 (2)	53.27 – 54.17	203.2 (8)	6/1/1987	Crushed Gravel	76.2 (3)	No subsurface drainage
I-394	6.52 - 7.64	254 (10)	10/1/1990	Gravel	76.2 (3)	Long. Drains

2.2 Distress survey

The distress type classifications used in this study were taken from MnDOT (2003) and the distress location measurement was taken from the FHWA distress manual (Miller and Bellinger, 2003). Distress type and locations are presented in Tables 2 and 3, respectively. According to Miller and Bellinger (2003) the distresses were classified regarding the degree of degradation in low (1), medium (2) and high (3) severity. The method developed allowed the research team to classify and record the location of 9 different distress types.

Table 2 - MnDOT distress classification

MnDOT #	MnDOT Distress Description
1	Transverse Joint Spalling
2	Longitudinal Joint Spalling
3	Faulted Joints
4	Cracked Panels
5	Broken Panels
6	Faulted Panels
7	Overlaid Panels
8	Patched Panels
9	Durability Cracking (D-Cracking)

Table 3 - Location of distressed areas in truck lane

Location #	Area	Distance from shoulder, m (ft)
Location 1	Right Edge	0.18 (0.6)
Location 2	Right Wheel Path	0.76 (2.5)
Location 3	Center	1.83 (6)
Location 4	Left Wheel Path	2.89 (9.5)
Location 5	Left Edge	3.47 (11.4)

MnDOT's Pavement Management Unit collects pictures of pavement condition using a Pathway Services Inc. Digital Inspection Vehicle (DIV). The data utilized in this study was generated by DIV and the Videolog software was provided to the research team by MnDOT. The Videolog software was used to process the data and provide the distress survey. The software is composed of four windows (Front View, Surface View, Location Window and Control Window), as shown in Figure 1. The software allowed for a more precise identification of each distress location, due to an interactive measurement tool on the software. The exact distance between the observed distress and the traverse was also recorded. To double check this imaging technique, distress were also recorded manually during the MIRA survey. Since transverse mid-panel cracking is expected in a JRCP, a slab was considered to be cracked if the transverse crack were of medium or high severity.

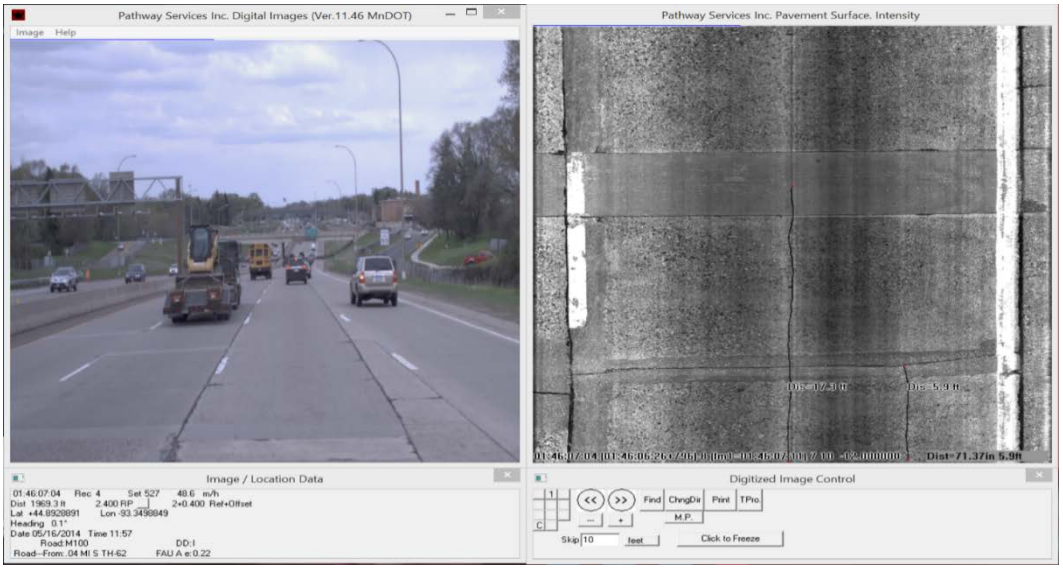

Figure 1 - Videolog Software showing one section of Highway100

2.3 Thickness survey

Various MIRA survey protocols were considered. These protocols explored differences in longitudinal and transverse measurement spacing. The key considerations in final protocol selection were hypothesized minimum scale of longitudinal and transverse variation and the time to implement the survey. A variogram analysis conducted by Vancura (2013) suggested spacing on the order of tens to hundreds of feet while Monte-Carlo modeling suggested that spacing of 4.5 m (15 ft) provided a statistically significant chance of detecting deviations from design thickness.

It was determined that longitudinal measurements every 3 m (10ft) with five transverse measurement locations spaced across the lane (Figure 2) would be sufficient to capture the longitudinal variation suggested by Vancura (2013) as well as explore traverse variation. Additionally, this geometry was chosen in an attempt to remain consistent with the transverse spacing outlined by Table 3 for distress location identification. This protocol also included performing all MIRA measurements as two closely spaced MIRA readings as a form of measurement verification. These measurements, referred to as a couple, were taken approximately 150 mm (6 in.) apart in the transverse direction. Readings were not taken within approximately 150 mm (6 in.) of joints or observable distress, as this was shown to cause issues with data processing. If a distress or joint was encountered at a measurement location, MIRA was offset to closest acceptable location.

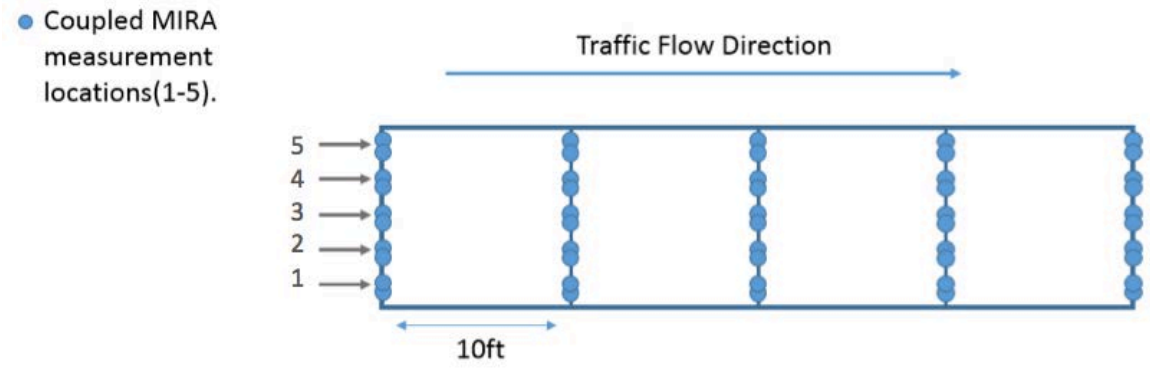

Figure 2 - MIRA measurement protocol

2.4 Data Processing

After MIRA surveys were completed, data processing was required. The end goal of data processing was to allow spatial relationship of thickness and velocity data to observed distress. Once the data was related, a statistical analysis could be performed. MATLAB was chosen to perform the spatial relation and statistical analysis.

First, the thickness and velocity measurements must be extracted from the data. This is done with application of an algorithm developed by Hoegh *et al.* (2011). The resulting output of the raw

Mira file processing is a file with thickness, shear wave velocity, and delay time measurements. After that the input thickness file for the MATLAB analysis could be created. This input file is a spreadsheet which contains important survey information which will be used in the data processing. The input file contains survey data including starting point, distance between longitudinal traverses, and number of readings per traverse.

The distress data required much less processing than the thickness data. Distress data regarding distress type, severity, traverse and distance from traverse was entered into a provided field data survey sheet which can be directly processed by MATLAB. During the combination of thickness/shear wave velocity and distress data, if couple thicknesses differ more than 6.35 mm (0.25 in.), this couple was considered as non-conclusive and the data for thickness and shear wave velocity was discarded from further analysis. Satisfactory couples were averaged, resulting in five transverse values to be associated with distress. As the MIRA data was taken at set intervals, and distress data was random, it was determined that MIRA locations would serve as base points and distress would be assigned to MIRA measurements. Specifically, a distress measurement occurring within +/- 5 ft. of a MIRA location was assigned to that MIRA data point (Figure 3). If a distress was recorded at exactly 5ft. from a MIRA location; that is, exactly between two measurements, it was at risk of being assigned to both or neither adjacent traverses. To avoid this, it was determined that a distress would only be associated with a MIRA measurement if the difference in longitude location d was $-5 > d \geq 5$ ft.

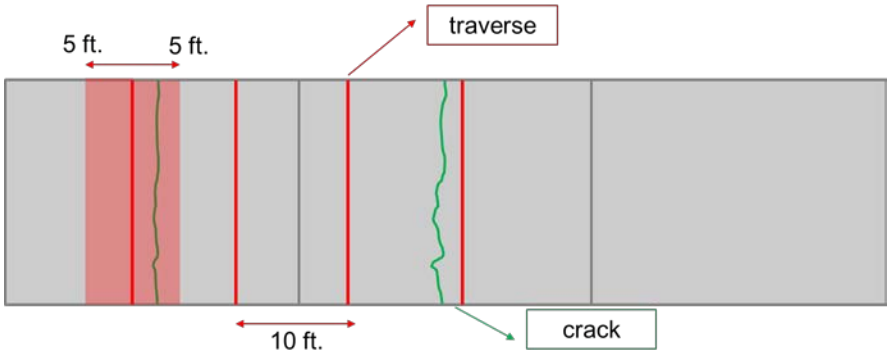

Figure 3 - Traverses and distress location

CHAPTER 3: STATISTICAL METHODOLOGY

This chapter describes the statistical analysis performed in the resulting combination of thickness and distress data.

3.1 Predictors

A primary goal of this study is correlation of thickness variation characteristics with observed distress. To achieve a thorough characterization of thickness variation, ten predictors (Table 4) were designed to exhaustively test all feasible thickness variation characteristics which could influence distress. Each one of these predictors resulted in one numeric value per traverse. A traverse, as described in section 2, is a transversal line of ultrasonic measurements containing five locations from the right edge to the longitudinal joint. Traverses are spaced in 3.0 m (10ft.) A basic description of the predictors are given below.

Table 4 - Thickness predictors

X_1	Average Traverse Thickness (mm)
X_2	Traverse Standard Deviation (mm)
X_3	Average traverse slope (mm/m)
X_4	Absolute Traverse Slope (mm/m)
X_5	Absolute Max traverse Slope (mm/m)
X_6	Maximum Absolute Difference in thickness (mm)
X_7	Sum of Critical Points (mm/m)
X_8	Largest Critical Point (mm/m)
X_9	Average Change in Traverse Slope (mm/m)
X_{10}	Average Longitudinal Slope (mm/m)

1. Average traverse thickness
   The average thickness per traverse is the arithmetic mean of the traverse measurements, determined by Equation 1, as follows:

$$t_{ave,i} = \frac{\sum_{j=1}^{m} t_{i,j}}{m} \quad (1)$$

   Where $t_{ave,i}$ is the calculated average thickness for the *ith* traverse, *m* is the number of measurements per traverse (5), and $t_{i,j}$ is the averaged couple thickness measurement.

2. Traverse Standard deviation

The traverse standard deviation is the sample standard deviation of the traverse measurements, determined by Equation 2, as follows:

$$std_i = \sqrt{\frac{\sum_{j=1}^{m}(t_{i,j} - t_{ave,i})^2}{m-1}} \quad (2)$$

Where std_i is the standard deviation of the *ith* traverse and *m* is the number of measurements within the traverse.

3. Average traverse slope
The average traverse slope is the difference in thickness between the start and end of the traverse, determined by Equation 3, as follows:

$$s_{i,k} = \frac{(t_{i,1} - t_{j,5})}{L_t} \quad (3)$$

Where $s_{i,k}$ is the traverse slope and L_t is the length of the traverse. Note that for a survey taken from right to left across the lane, a positive slope indicates decreasing thickness from right to left, while a negative slope indicates increasing thickness from right to left.

4. Absolute traverse slope
To explore the significance of overall degree of slope along a traverse, and to eliminate the influence of slope direction, the absolute slope was calculated by Equation 4 and Equation 5, as follows:

$$s_{i,k} = \frac{(t_{i,j} - t_{j+1})}{L_c} \quad (4)$$

Where $s_{i,k}$ is the traverse slope between adjacent couples and L_c is the distance between the couples. The overall degree of slope is then calculated (Equation 5) by summing the absolute values of the slopes between couples:

$$sAbs_{ave,i} = \frac{\sum_{i=1}^{k} abs(s_{i,k})}{m} \quad (5)$$

Where, $sAbs_{ave,i}$ is the average slope of the traverse.

5. Absolute max traverse slope
To explore the effect of the high degrees of slope, the absolute maximum slope per traverse was computed. This predictor returns the largest magnitude of slope, whether positive or negative while maintaining the sign of the slope. The predictor is determined by Equation 6.

$$st_{MAX,i} = \text{MAX}\big(abs(s_{i,k})\big) \quad (6)$$

Where $st_{MAX,i}$ is the absolute max traverse slope. The sign associated with the maximum absolute value is then reassigned to the highest magnitude slope found.

6. Maximum absolute difference in thickness

The maximum absolute difference in thickness along a traverse was computed by comparing the maximum and minimum thickness within each traverse using Equation 7, as follows:

$$maxAbsDiff_i = \text{abs}\left(\text{MAX}\left(t_{i,j}\right) - MIN\left(t_{i,j}\right)\right) \quad (7)$$

Where $maxAbsDiff_i$ is the maximum absolute difference in thickness, $\text{MAX}\left(t_{i,j}\right)$ is the maximum thickness along the traverse, and $MIN\left(t_{i,j}\right)$ is the minimum thickness in the traverse.

Changes from positive to negative slopes, referred to as critical points, were assumed to have potential to create stress concentrations. To investigate the effect of critical points, two predictors were calculated. The first was the sum of the slope changes of all the critical points within each traverse. The second was the slope change of the maximum critical point. The presence of a critical point was determined by comparing adjacent slopes (Equation 8). If the product of the slopes is negative, the sign of the slope has changed, and a critical point exists. A maximum of three critical points could occur along one traverse.

$$Logical_{cp}, i = if\left(s_{i,k} * s_{i,k+1}\right) < 0 = TRUE \quad (8)$$

In locations where a critical point was found, the magnitude of the critical point was determined by comparing the change in slope by Equation 9, as follows:

$$CP_i = abs(s_{i,j}) + abs\left(s_{i+1,j}\right) \quad (9)$$

Where CP is the magnitude of the critical point, $s_{i,j}$ is the traverse slope

7. Sum of critical points

To explore the cumulative effects of multiple critical points, the magnitude of all critical points occurring on a traverse were summed using Equation 10, as follows:

$$sumCrit_i = \sum_{i=1}^{l} CP_i \quad (10)$$

Where $sumCrit_i$ is the sum of all the critical points occurring within the traverse.

8. Largest critical point

The effect of the largest magnitude of critical point was also of interest. The maximum critical point was determined using Equation 11, as follows:

$$largestCrit_i = MAX(CP_i) \quad (11)$$

Where $largestCrit$ is the largest critical point within the traverse.

9. Average change in traverse slope

To explore the effects of the change in traverse slope between adjacent traverses, the average change in traverse slope was calculated by Equation 12, as follows:

$$aveChngTrvSlope_i = s_{ave,i} - s_{ave,i+1} \quad (12)$$

Where $aveChngTrvSlope_i$ is the difference in slope between adjacent traverse.

10. Average longitudinal slope

To explore the effects of the longitudinal slope, the absolute average longitudinal slope was calculated (Equation 13) by comparing the change in the average thickness of adjacent traverses.

$$aveLongSlope_i = abs\left(\frac{(t_{ave,i} - t_{ave,i+1})}{d_l}\right) \quad (13)$$

Where $aveLongSlope_i$ is the average longitudinal slope, $t_{ave,i}$ is the average thickness of the traverse, and d_l is the longitudinal distance between traverses.

3.2 Logistic Model

Logistic regression was used to determine correlation of predictors and distress. Unless otherwise noted, all implementation of the logistic regression model was taken from Hosmer et al (2013). All analysis was performed in MATLAB®. Logistic regression is useful when estimating the probability of a binary response; in this case, the occurrence or non-occurrence of distress. A logistic model was employed to test the significance of the proposed regressors. The logistic regression is a transform of the linear one regressor model. The linear model is given by Equation 14, as follows:

$$E(Y|x) = \pi(x) = \beta_0 + \beta_1 x \quad (14)$$

Where $E(Y|x)/\pi(x)$ is the expected value of Y given *x*, β_0 is the fit intercept term and β_1 is the value of the linear term.

The transformation applied for the logistic model is the logit, and is given by Equation 15 and 16, as follows:

$$logit(x) = \log\left[\frac{\pi(x)}{1-\pi(x)}\right] = \beta_0 + \beta_1 x \quad (15)$$

Therefore, the predicted probability can be solved for as follows:

$$\pi(x) = \frac{e^{\beta_0 + \beta_1 x}}{1 + e^{\beta_0 + \beta_1 x}} \quad (16)$$

The logit transformation (Equation 14) preserves many of the desirable properties of a linear regression model and the principals which guide linear regression analysis apply to logistic regression. The logit is linear in its parameters, may be continuous, and may range from $-\infty$ to

+∞. The logistic regression model is bounded by 0 and 1 and is therefore valid for estimating probabilities. Unlike the linear regression model, the errors associated with the logistic regression model are binomially rather than normally distributed.

3.3 Fitting the Logistic Model

The unknown parameters β_0 and β_1 of the logistic regression are estimated by maximizing the likelihood function. Maximizing the likelihood function yields the values for the unknown parameters which maximize the probability of the observations. The likelihood function is given by Equations 17 and 18, as follows:

$$l(\boldsymbol{\beta}) = \prod_{i=1}^{n} \pi(x_i)^{y_i}[1 - \pi(x_i)]^{1-y_i} \tag{17}$$

Where $\pi(x_i)$ is the *ith* predicted probability associated with the *ith* regressor, y_i is the *ith* response, and $\boldsymbol{\beta}$ is the fit regression terms given by equation 18, as follows:

$$\boldsymbol{\beta} = \beta_0 + \beta_1 \tag{18}$$

Mathematically, it is easier to use the log of the function, referred to as the log-likelihood function. To find the value of $\boldsymbol{\beta}$ that maximizes the likelihood function, the function is differentiated with respect to β_0 and β_1 and set equal to zero. The log likelihood is given by Equation 19, as follows:

$$L(\boldsymbol{\beta}) = log(l(\boldsymbol{\beta})) = \sum_{i=1}^{n}\{y_i \log\big(\pi(x_i)\big) + (y_i - 1)log\big(1 - \pi(x_i)\big)\} \tag{19}$$

3.4 Significance of Fit Parameters

The first step in evaluating the model is testing the fit coefficients $\boldsymbol{\beta}$ for statistical significance. This is performed with the likelihood ratio test. The likelihood ratio, or G statistic, is testing if the model which includes fit coefficients tells us more about the outcome variable than the model which does not include the fit coefficients. The likelihood is determined by taking the log of the ratio of the likelihood of the model without the test parameter over the fit maximized likelihood of the model with the parameter. If this value is large, the fit model is much better than the model without the test parameter.

The results of this comparison can be used to formulate a hypothesis test. For the two parameter regression (β_0 and β_1) regression performed, *G* follows a chi-squared distribution with 1 degree of freedom.

To test the significance of β_1, Equations 20 and 21 are applied:

$h_0: \hat{\beta}_1 = 0$

$h_1: \hat{\beta}_1 \neq 0$

$$G = -2 * ln\left(\frac{likelihood\ without\ the\ variable}{likelihood\ with\ the\ variable}\right) =$$
$$2 * \{ln(likelihood\ with\ the\ variable) - \ln(likelihood\ without\ the\ variable)\} \quad (20)$$

The results of the G statistic can be used to calculate a p-value as follows:

$$p - value = P(\chi^2(1)| > G) \quad (21)$$
$$\alpha = 0.05$$

An $\alpha = 0.05$ denotes the probability of the rejecting the null hypothesis (that there is no correlation) when it is true. At $\alpha = 0.05$, there is only a 5% chance of claiming correlation when none exists.

CHAPTER 4: PRELIMINARY RESULTS

The summary of thickness measurements are presented in in Table 5. Only I-394 presented an average thickness higher than the design thickness (positive thickness difference). The other three projects presented an average thickness deficiency. A lower coefficient of variation indicates a consistent dataset with less variability compared to the mean.

The last two lines in Table 5 presents information on maximum thickness difference within a traverse and in between consecutive traverses, respectively. Since the distance from the first and last measurement couple in a traverse is 3.2 m (10.5 ft.) and the distance between traverses is 3 m (10 ft.) the results imply in similar variation of thickness in transverse and longitudinal direction with the longitudinal thickness difference being slightly greater.

Table 5 - Thickness characteristics

	Highway 60 East	Highway 60 West	Highway 100	I-394
# Measurements	2000	3000	1530	2000
# Traverses	200	300	153	200
Design Thickness (mm)	203.2	203.2	228.6	254
Avg. Thickness (mm)	195.81	199.57	220.17	259.35
Std. dev.	10.03	10.86	10.87	10.17
Coef. of Variation	0.0512	0.0544	0.0494	0.0394
Avg. Diff. from Design Thickness (mm)	-7.39	-3.63	-8.43	5.35
Max. Thickness (mm)	225.40	234.44	250.00	286.63
Min. Thickness (mm)	164.16	170.18	200.00	216.43
Max. Traverse Thickness Diff. (mm)	32.63	35.14	43.48	30.36
Max. Long. Thickness Diff. (mm)	35.14	43.67	50.00	39.04

Regarding the thickness transverse variation, all sections, save I-394, present greater thickness in the lane left edge of the slab than the right, as can be seen in Figure 4. Moreover, all sections have thinner slabs closer to the right edge. Locations 1 to 5 are based on the distress locations provided in Table 3.

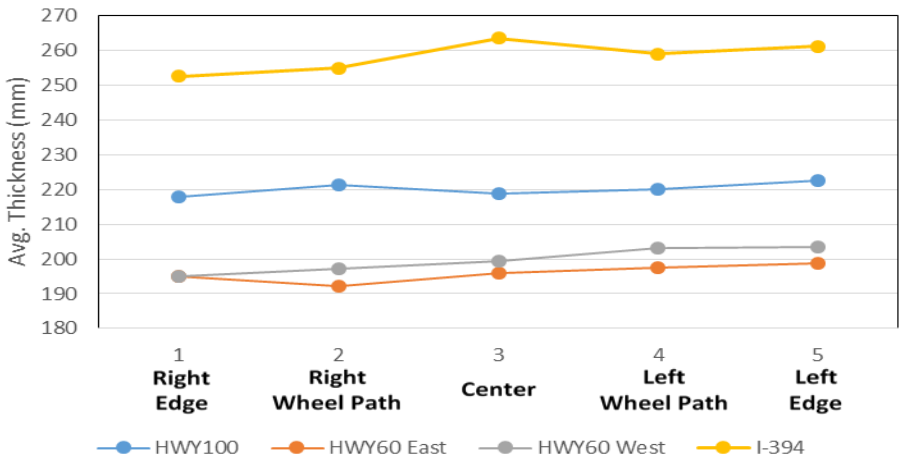

Figure 4 – Average thickness per location

4.1 Observed surface distresses

Table 6 summarizes the number of observed surface distresses and the percentage of affected traverses. About 50% of the analyzed traverses show one or more performance failures. Joint spalling seems to be common distress for all sections while faulting and D-Cracking were not significantly observed. As can be seen, Highway 60 presents a greater number of cracked or broken (Figure 5) panels than the other sections. It is also interestingly to note that although Highway 100 section has the highest thickness deficiency (i.e. difference between design and average measured thicknesses) it exhibited a significantly smaller percentage of cracked or broken panels at the end of the service life. The rehabilitation of this section was actually triggered by joint spalling. At the same time, the I-394 pavement as-built thickness was on average greater than the design thickness, but the pavement still exhibited a large number of overlaid or patched panels. Moreover, joint spalling (transverse and longitudinal – Figure 6) seems to be common distresses for all sections while faulting and D-Cracking were not significantly observed.

Table 6 - Compilation of observed surface distresses

DISTRESSES	AFFECTED TRAVERSES							
	Highway 60E		Highway 60W		Highway 100		I-394	
	#	%	#	%	#	%	#	%
Transverse Joint spalling	40	20	30	10	22	14.38	32	16
Longitudinal joint spalling	25	12.5	14	4.67	50	32.68	27	13.5
Faulted joint	0	0	1	0.33	0	0	1	0.5
Faulted crack	0	0	1	0.33	0	0	0	0
Cracked or broken panel	57	28.5	95	31.67	13	8.5	7	3.5
Overlaid or patched panel	11	5.5	16	5.33	4	2.61	29	14.5
Durability (D) cracking	0	0	0	0	0	0	0	0
All distress	90	45	135	45	77	50.33	89	44.5

Figure 5 - Broken panels in Highway 60 East

(a) (b)

Figure 6 - (a) Transverse joint spalling in I-394 and (b) longitudinal joint spalling in Highway 60 East

4.2 Concrete condition

In order to determine the level of damage present in concrete slabs in a quantitative and non-subjective manner, a novel method of MIRA signal interpretation called the Hilbert Transform Indicator (HTI) was utilized for slab characterization. This indicator is based upon the signal characteristics which sound concrete exhibits, allowing for variations from this condition to be seen numerically. The value is shown below in mathematical form in Equation 21:

$$HTI = \int_0^{500} \frac{HT(t)}{\max(HT(t))}\, dt \tag{21}$$

Where HT(t) is the Hilbert transform envelope. A higher HTI value would be indicative of damaged concrete, while a low value represents sound concrete. This is due to the increased oscillation in the signal present for damaged concrete conditions, which increases the

instantaneous amplitude envelope. In general, values below 90 are regarded as an indicator of sound concrete while values above 100 indicate the initial development of damage. Extensive damage results in HTI values in the range of 120-160. The HTI was proved to correctly identify concrete condition even if distresses are not visible on the slab surface (Freeseman, *et al.*, 2016a).

Average HTI for section Highway 60 East and West was 69 and 70, respectively, while for sections Highway 100 and I-394 it was 79 and 66, i. e., all sections exhibit a sound concrete condition. Some points in Highway 100 presented values above 90 with most of these locations also presenting distresses. However a correlation between distresses and HTI was not conclusive. The lack of relationship between distresses and HTI can be explained by the distress survey methodology. The survey method recorded distresses within a range of 5 ft. of the traverse location, while the HTI only assessed concrete condition for the exact position of the measurement.

CHAPTER 5: COMBINED RESULTS

This chapter presents the resulting combination of distress and thickness/shear wave velocity data for each of the surveys.

5.1 Highway 60 (Highway 60)

Figure 7 shows the results of MIRA-determined thickness and SWV measurements as well as distresses along the Highway 60 East section. The axis "traverse location" denotes the 1 to 5 locations of the couple measurements according to Figure 1. The "stationing" axis corresponds to the length of survey completed with each traverse spaced approximately 3 m (10 ft.) from the next one. The grey contoured surface depicts thickness in the upper map (Figure 7a) and SWV in the lower map (Figure 7b). Areas with a darker grey indicate a thicker slab or greater SWV values. Blank spots in the contoured surface denote a couple error (non-conclusive results). Figure 7c displays the distress survey. Each distress is represented by a corresponding symbol.

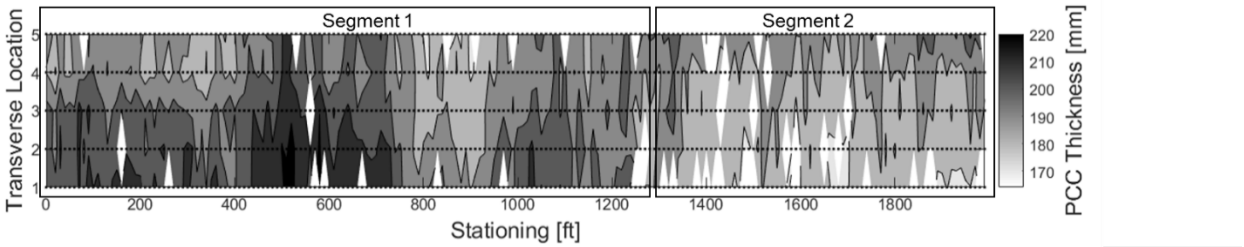

(a) Thickness map

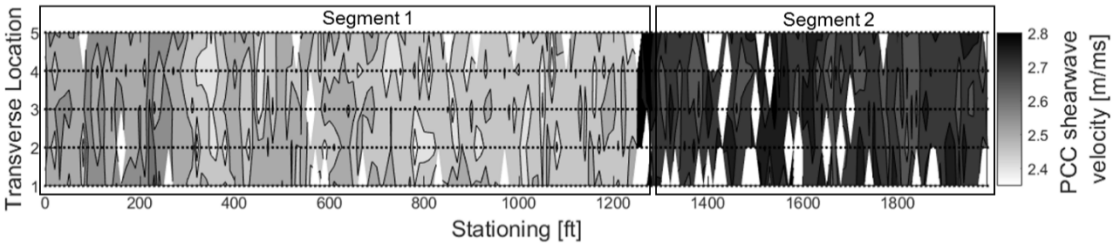

(b) SWV map

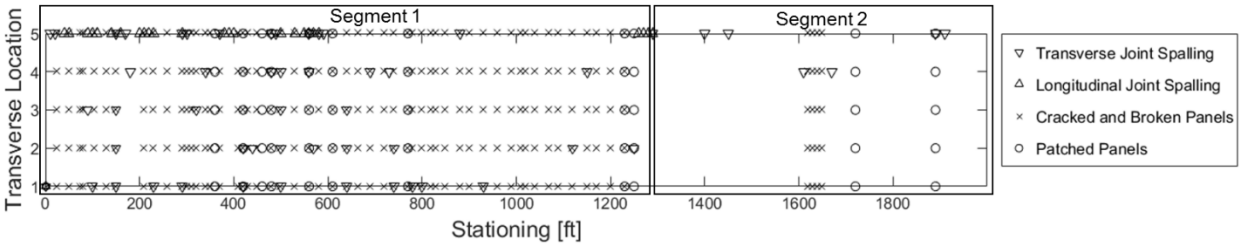

(c) Distress map

Figure 7 - Highway 60 East survey of (a) thickness, (b) SWV and (c) distresses.

An analysis of the surface distress map shown in Figure 7c reveals that there is a change in pavement performance around the 1250 ft. station. A higher density of distresses was observed between stations 0 ft and 1250 ft than between stations 1250 ft and 2000 ft. Examination of thickness variability between those two segments show that the most damaged segment (1, station 0 ft. to 1250 ft.) presents an average thickness of 200 mm (7.87 in.) while the less damaged segment (2, station 1260 to 2000 ft.) shows a 12 mm (0.47) thinner slab. The segments are also clearly defined in the SWV plot. There is a great rise in SWV after station 1250 ft. The average SWV increased from 2.49 m/ms in segment 1 to 2.72 m/ms in segment 2.

For a combined survey visualization, Figure 8 presents the two dimensional outlook of both velocity and thickness *versus* distresses. The dashed horizontal black line denotes the design thickness. Thickness fluctuations between stations 400 and 1000 ft. do not seem to have an impact on the presence or lack of surface distresses as the SWV in this segment presents small variations. It is only when the SWV rises (after station 1200 ft.) that there is a discontinuity of the major distresses affecting the previous traverses. Counterintuitively, the less damaged segment presents thickness below the design thickness. This suggests that variations in SWV are more influential on pavement performance than variations in thickness for this pavement section.

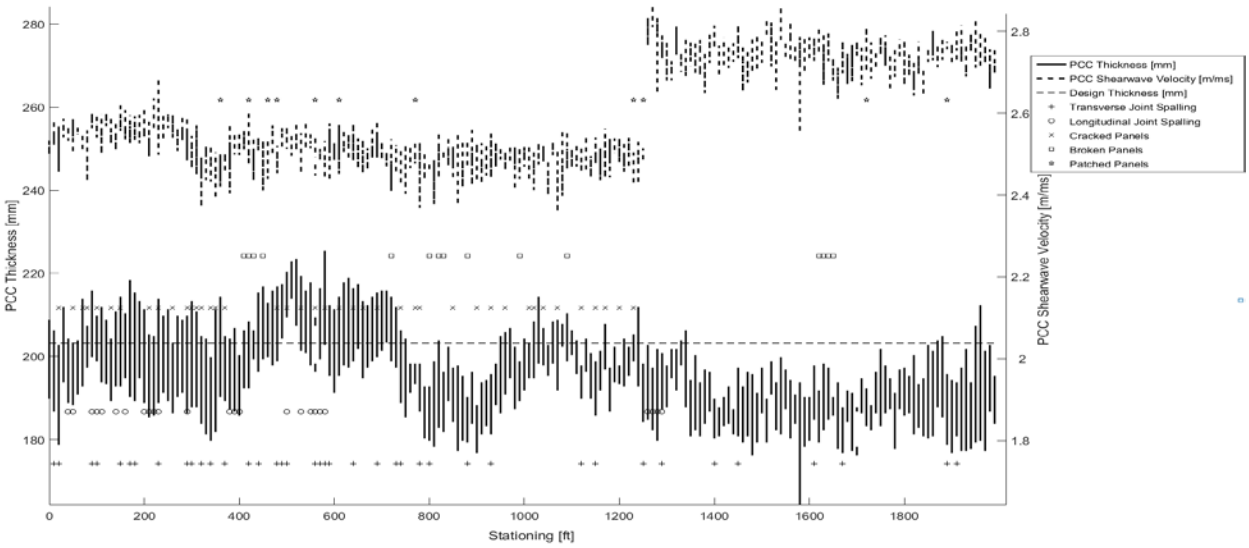

Figure 8 - Combination of Highway 60 East results.

The survey conducted on Highway 60E started on the east direction slightly before MP53 covering over 1900 ft. Once finished, the survey team changed lanes and moved in the opposite direction (West survey), surveying approximately 3000 ft.

For Highway 60 West, results are shown in Figure 9. Again, there is a clear drop in SWV around the 440 ft. station so two distinguished segments can be identified: segment 3 located between stations 0 ft and 440 ft and segment 4 located between stations 440 ft and 3000 ft.

Segment 3 exhibited a higher velocity compared to segment 4, 2.76 vs. 2.52 m/ms, respectively. At the same time, segment 3 exhibited a lower density of distresses compared to segment 4, while the difference in thickness increased from 186 to 202 mm (7.32 to 7.95 in.). Figure 10 further attest this findings.

An analysis of the construction records revealed that this part of Highway 60 was constructed in two stages eight months apart. The first stage covered segments 1 and 4, while the second stage covered segments 2 and 3. Slightly different concrete mixes were used for each stage. Table 7 highlights the differences in concrete mixture design between the two segments.

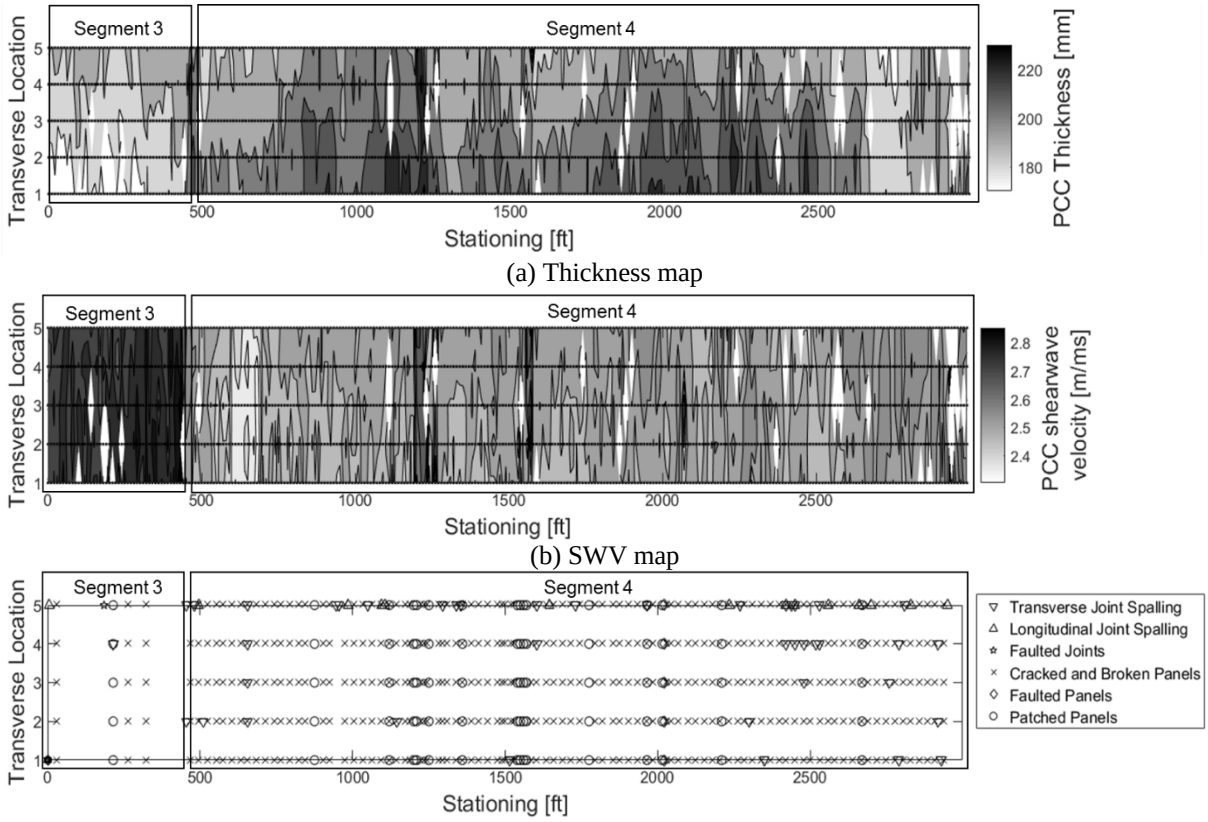

(a) Thickness map

(b) SWV map

(c) Distress Map

Figure 9 - Highway 60 West survey of (a) thickness, (b) SWV and (c) distresses.

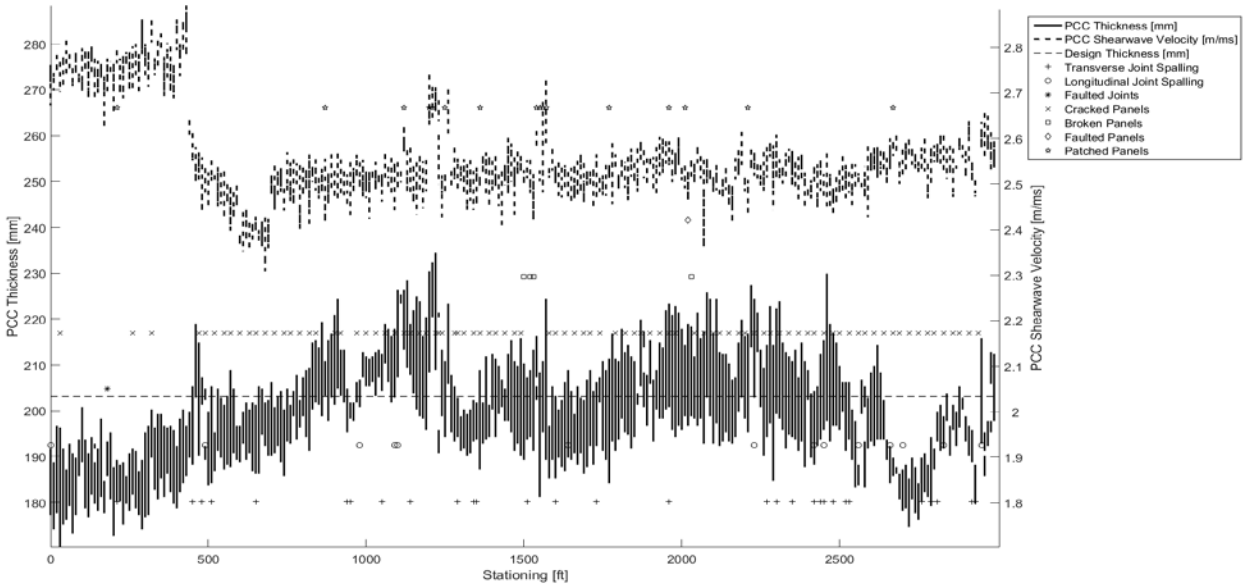

Figure 10 - Combination of Highway 60 West results

Table 7 - Concrete mixture design for segments 1 and 2 in Highway 60

	Mix design (lb/yd$^{3)}$	
	Stage 1 (Segments 1 and 4)	Stage 2 (Segments 2 and 3)
Coarse Agg.	1791	1858
Fine Agg.	1200	1200
Cement	472	451
Water	260	240
Flyash	83	79
Coarse Aggregate Source - Type	Northern ConAgg (167001) - Gravel/crushed New Ulm Quartz (152003) – Gravel	New Ulm Quartz (152003) - Crushed - Quartzite/Granit
Coarse Agg. Size (in.)	2	2

Table 7 shows that the Stage 1 concrete mix has more cement content while having less coarse aggregate. A higher level of cement content may imply higher shrinkage stress, explaining the greater number of cracks in segments 1 and 4. The coarse aggregate source could also help elucidate the diverse performance, as some aggregates present higher coefficient of thermal expansion which can be detrimental for the concrete performance. Information regarding the aggregates used in Stage 1 disclosed that MnDOT no longer allows the use of Northern ConAgg (167001) aggregate in new concrete pavements because of durability issues related to high levels of carbonate (41.32 to 55.8 %) within the aggregate. As Stage 1 had a 50/50 mix of both coarse aggregates, the poor performance indicates that mixing good quality aggregate with bad quality aggregate does not mask the latter's performance.

Core data taken after the section construction shows a thinner slab for segment 2 in accordance to the MIRA data. However, the average thickness of cores for both segments was higher than the design thickness. Average core thickness for segment 1 is 218 mm (8.57 in.) while segment 2 is 211 mm (8.3 in.).

5.2 Highway 100 (Highway 100)

For Highway 100, there is an increase in SWV (around the station 700 ft. in Figure 11b) which corresponds to an area with the presence of cracked panels (Figure 11c) in contrast with the results of Highway 60. Yet, this higher velocity becomes quasi-constant through the survey, including the next area with less distresses. After station 700 ft., the average velocity rises from 2.58 to 2.73 m/ms while the average thickness remains relatively constant around 220 mm. It can be observed that around the cracked area there is also a corresponding great number of thickness couple measurement errors (Figure 11a). As the data procedure eliminates thickness and SWV data whenever a thickness error occurs, the cracked panels presented in this particular area could not be related to the SWV. Additionally, the number of measurement errors in that particular area can be an indicator of distresses within the slab, making it difficult for a consistent thickness determination. The graph on Figure 12 supports this information.

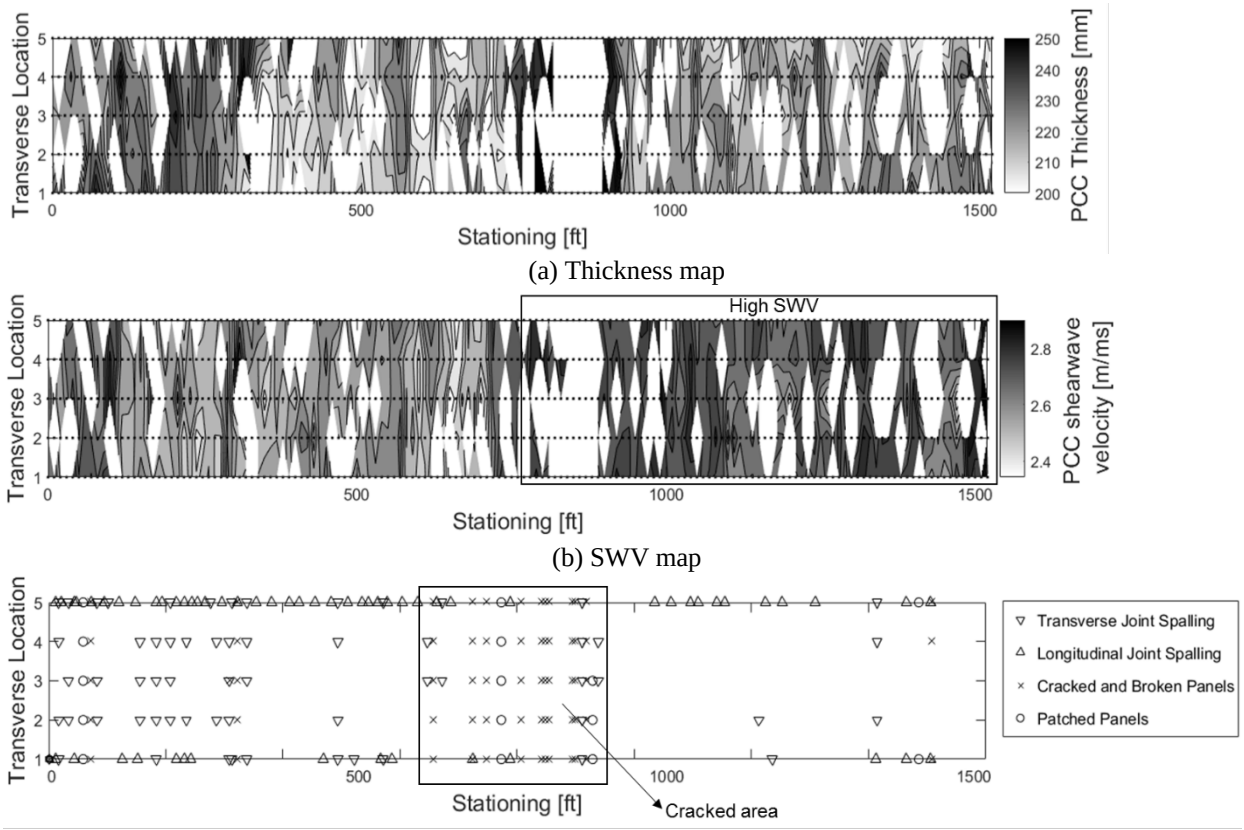

(a) Thickness map

(b) SWV map

(c) Distress map

Figure 11 - Highway 100 survey of (a) thickness, (b) SWV and (c) distresses.

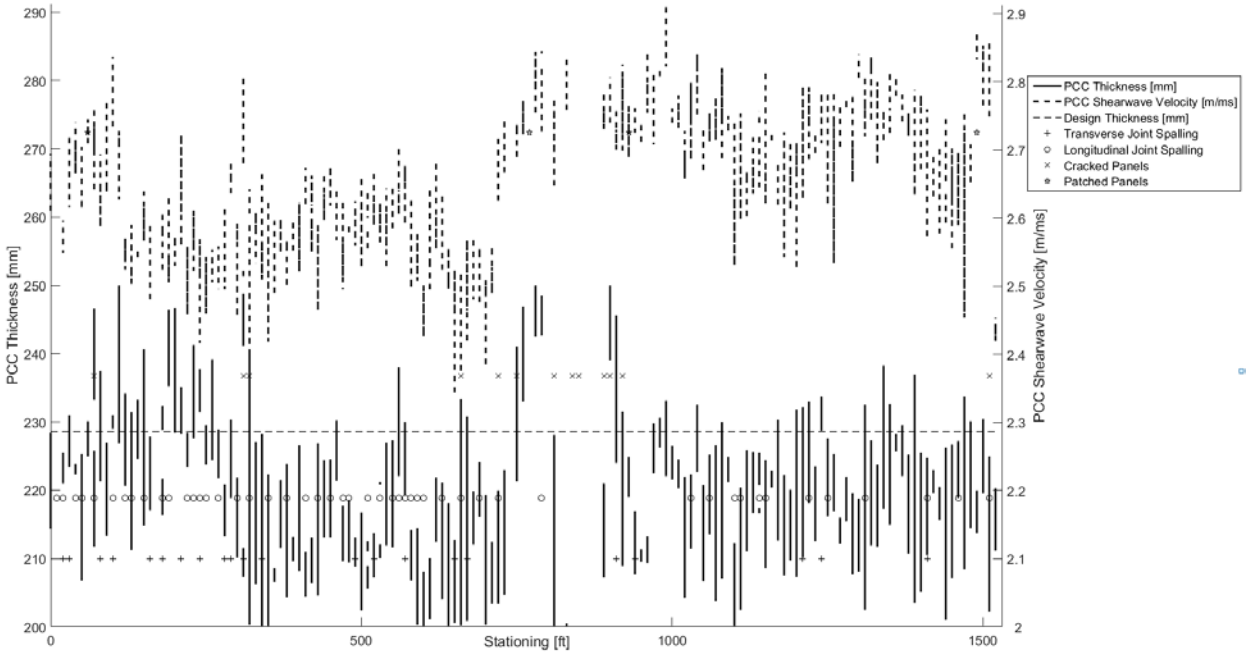

Figure 12 - Combination of Highway 100 results

5.3 Interstate 394 (I-394)

Figures 13 and 14 show much less variation for thickness and especially for SWV (average of 2.76 m/ms) for I-394, than the other sections. I-394 has a great number of patched panels. Information on distress type prior to rehabilitation was not found within MnDOT. There is an area, around stations 1100 and 1600 with much less patched panels. However, no significant changes in thickness or velocity were observed for this segment.

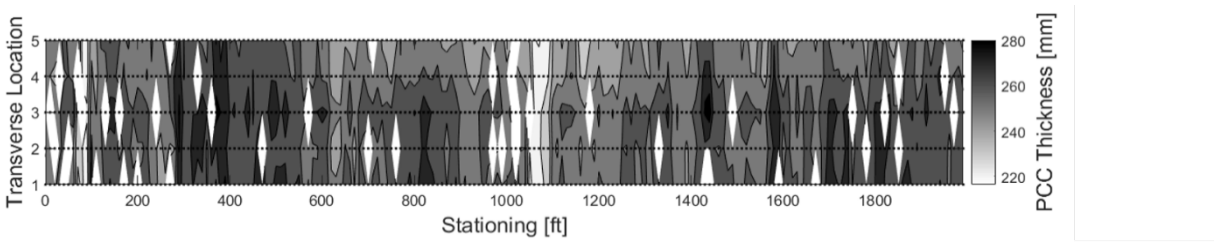

(a) Thickness map

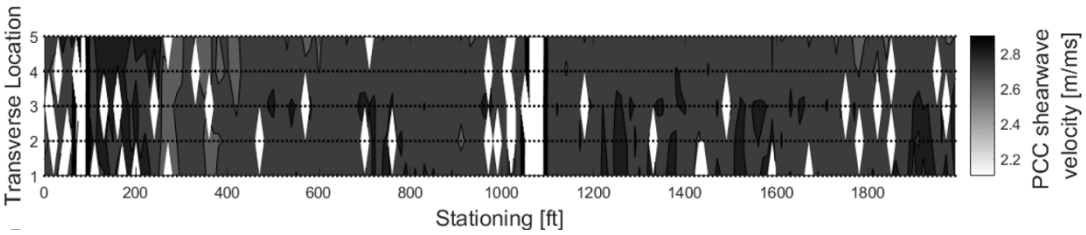

(b) SWV map

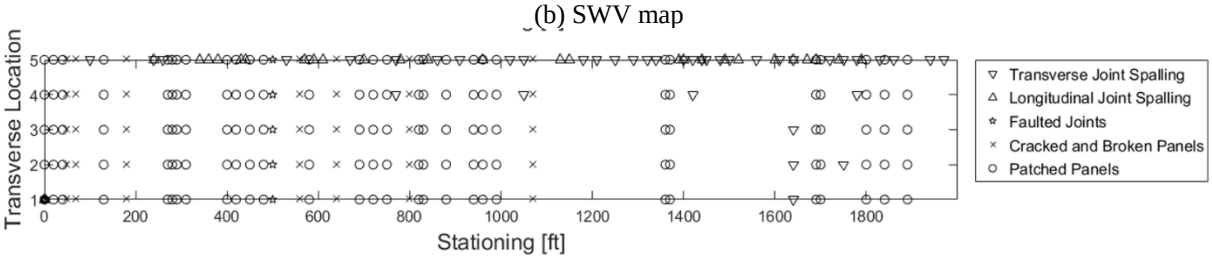

(c) Distress map

Figure 13 - I-394 survey of (a) thickness, (b) SWV and (c) distresses.

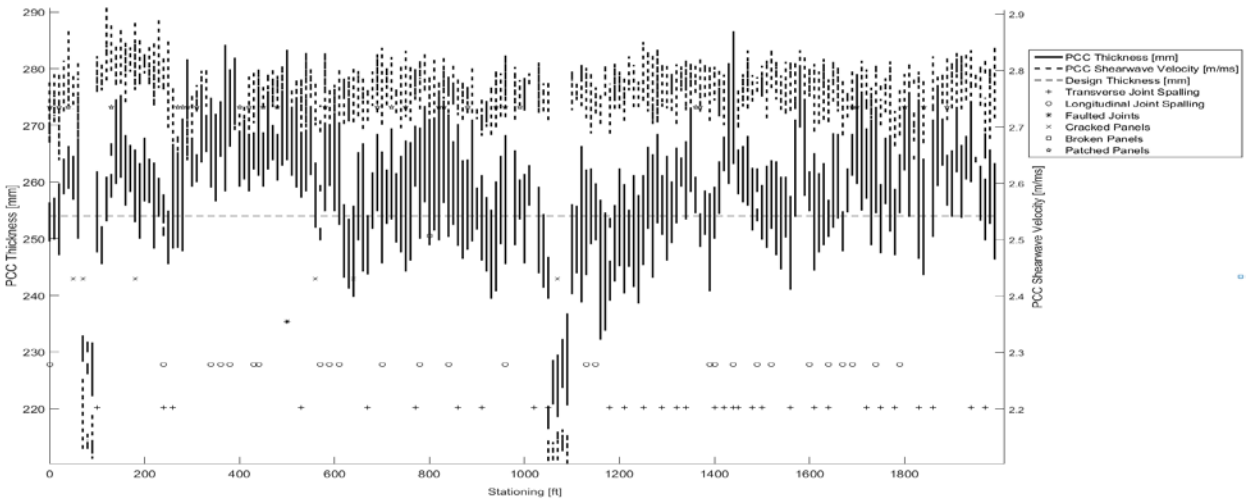

Figure 14 - Combination of I-394 results

CHAPTER 6: REGRESSION RESULTS

The visual analysis performed on the plots above suggests some interesting relationships. To further explore any correlations, a formal statistical analysis was performed. The regression analysis performed on thickness and velocity produced several interesting results, but also revealed some limitations of the data sets. A main issue encountered was the lack of consistency of distress profiles across the surveys. For example, Highway 60 East contains 57 cracked or broken panels (28.5% of the total slabs) while I-394 contains only 7 cracked or broken panels (3.5% of the total slabs). If a significant correlation were found between a predictor and cracked and broken panels, it is extremely unlikely that I-394 would yield the same relationship due to its lack of cracked and broken panels.

Ideally, a significant correlation would be found between a predictor and distress across all four surveys. Such an ideal correlation would suggest that the predictor can be correlated with a distress type in various pavement designs. However, the inconsistency of distress profiles between datasets suggests that finding the same significant correlation across all four surveys is very unlikely. To address this issue, only the correlation results of datasets with similar distress profiles will be compared. Additionally, correlations will be limited to distress types which were dominant (greater than 10% of total distress) in at least two surveys. These distress types include traverse joint spalling, longitudinal joint spalling, cracked and broken panels, and all distress types.

6.1 Thickness statistical analysis

- Traverse Joint Spalling

Traverse joint spalling accounted for 10-20% of distress in the surveys. Though the traverse joint spalling was found to significantly relate to several thickness predictors in Highway 60 East and one predictor on I-394, the correlations were not strong and were not consistent across surveys (Table 8). Additionally, some of the correlations found on Highway 60 East, such as an increase in distress occurrence with increasing thickness, were counter intuitive and unreasonable. Therefore, it is assumed that there is no correlation between thickness variability and traverse joint spalling.

- Longitudinal Joint Spalling

Longitudinal joint spalling accounted for 5% to 33% of distress in the surveys. Longitudinal joint spalling was found to be significantly related to several thickness predictors in Highway 60 East and one predictor in Highway 100. However, as with traverse joint spalling, correlations were not strong and were not consistent across surveys (Table 8).

- Cracked and Broken Panels

Though cracked and broken panels only accounted for a small percentage of the distress in the Highway 100 (8.5%) and I-394 (3.5%), it was the main distress type for Highway 60 East (28.5%) and Highway 60 West (31.7%). Therefore, Highway 60 East and Highway 60 West

datasets will be compared. Cracked and broken panels were found to significantly relate to several thickness predictors. There was a strong negative correlation ($p < 0.005$) found between cracked and broken panel occurrence and average traverse slope (X_3) (Figure 15) and absolute maximum traverse slope (X_5) (Figure 16) in Highway 60 East. Both of these correlations suggest that pavements with a negative thickness slope (thickness increasing from right edge to left) are more likely to exhibit cracked or broken panels. This relationship can be also verified for Highway 60 West (Figures 17 and 18).

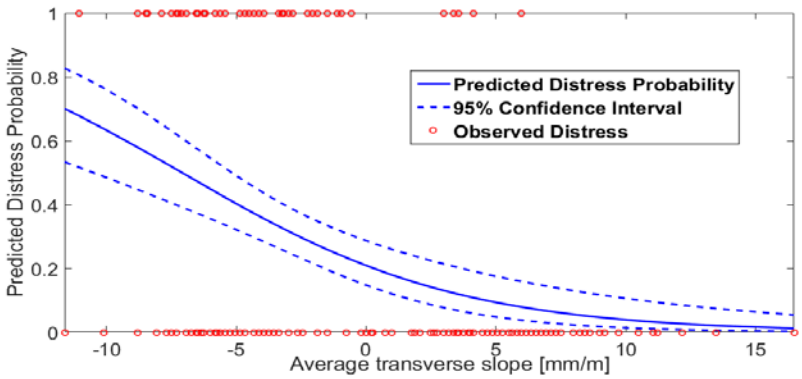

Figure 15 - Highway 60 East (Thickness): Average Traverse Slope *versus* Cracked and Broken Panels.

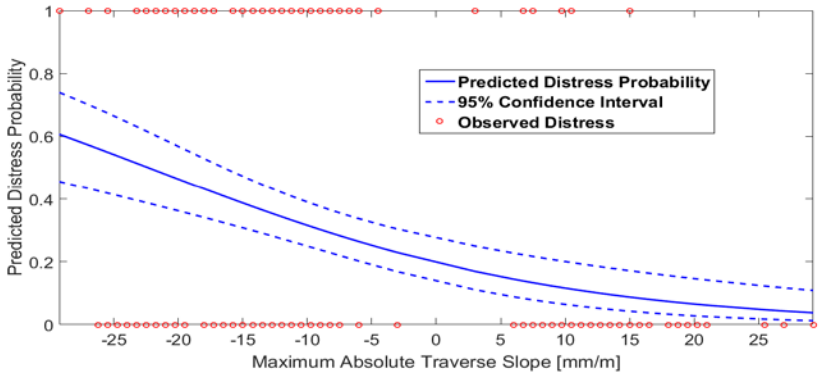

Figure 16 - Highway 60 East (Thickness): Absolute Maximum Traverse Slope *versus* Cracked and Broken Panels.

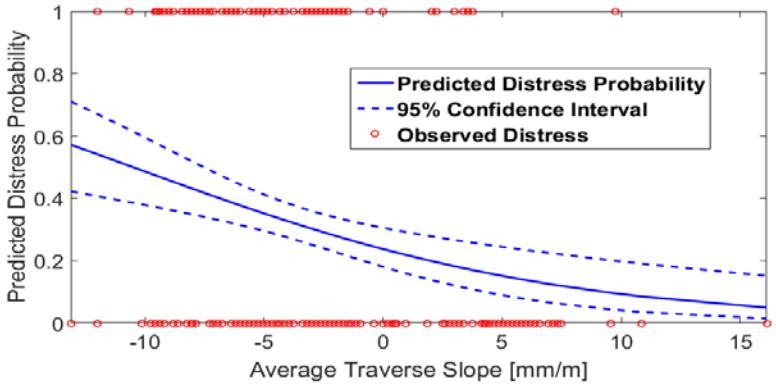

Figure 17 - Highway 60 West (Thickness): Average Traverse Slope *versus* Cracked and Broken Panel.

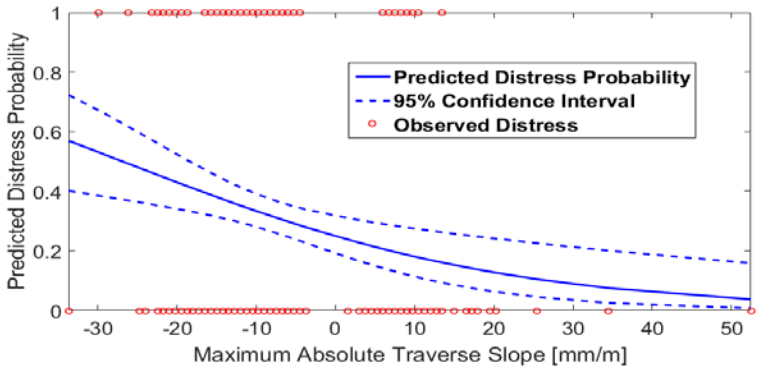

Figure 18 - Highway 60 West (Thickness): Absolute Maximum Traverse Slope *versus* Cracked and Broken panels.

- All distress

All distress allows datasets with different distress profiles to be compared. This helps adjust for human bias in recording and may allow the detection of correlations that may not be significant in a single distress type, but are relevant for overall pavement quality. The analysis of all distress revealed no new correlations. The strong negative correlations between traverse slope and cracked and broken still leads the correlation and provides no new information (Table 8).

Table 8 - Pavement thickness variation and distress correlation

		HWY 60E		HWY 60W		HWY 100		I 394	
		Coeff[a]	Sig[b]	Coeff[a]	Sig[b]	Coeff[a]	Sig[b]	Coeff[a]	Sig[b]
Transverse Joint Spalling	X_1	0.0430	0.0489	-0.0011	0.9575	0.0234	0.3591	-0.0160	0.4615
	X_2	0.1911	0.0168	-0.0816	0.2999	-0.0239	0.6509	0.1281	0.1045
	X_3	-0.1051	0.0021	-0.0402	0.3407	0.0107	0.7150	-0.0089	0.8712
	X_4	0.1043	0.1081	-0.0421	0.5834	-0.0151	0.7038	-0.0327	0.5795
	X_5	-0.0333	0.0110	-0.0319	0.0930	-0.0139	0.3207	0.0001	0.9970
	X_6	0.0726	0.0275	-0.0438	0.1890	-0.0134	0.6239	0.0418	0.2550
	X_7	0.0174	0.2046	0.0118	0.4959	-0.0167	0.3247	-0.0439	0.0030
	X_8	0.0411	0.1000	0.0039	0.8927	0.0065	0.8089	-0.0294	0.2770
	X_9	0.0213	0.7987	-0.0773	0.4339	0.0311	0.3282	0.0491	0.4876
	X_{10}	0.1430	0.6298	-0.0609	0.8037	0.0969	0.4515	0.2586	0.0728
Longitudinal Joint Spalling	X_1	0.0898	0.0008	0.0034	0.9097	0.0190	0.3276	0.0291	0.2712
	X_2	0.3372	0.0006	0.1057	0.3212	-0.0239	0.5354	-0.1271	0.1837
	X_3	-0.1038	0.0132	0.0009	0.9871	0.0779	0.0022	0.0140	0.8068
	X_4	0.1986	0.0093	-0.1341	0.2541	-0.0007	0.9802	-0.0016	0.9795
	X_5	-0.0596	0.0007	0.0009	0.9696	0.0190	0.0685	0.0148	0.3642
	X_6	0.1071	0.0065	0.0163	0.7207	-0.0003	0.9896	-0.0382	0.3593
	X_7	0.0364	0.0198	-0.0256	0.3881	0.0035	0.7595	-0.0232	0.1196
	X_8	0.0808	0.0081	0.0645	0.0585	-0.0179	0.4003	-0.0167	0.5445
	X_9	0.0824	0.3779	0.1043	0.3119	-0.0332	0.2493	0.0864	0.2334
	X_{10}	0.2402	0.4945	-0.1148	0.7488	-0.1355	0.2382	-0.3005	0.1911
Cracked and Broken Panels	X_1	0.0532	0.0067	0.0245	0.0755	0.0199	0.5343	-0.0755	0.0259
	X_2	0.0551	0.4346	0.0453	0.3606	0.0883	0.0771	0.0912	0.5578
	X_3	**-0.1877**	**0.0000**	**-0.0931**	**0.0009**	0.0393	0.2829	0.0454	0.6608
	X_4	-0.0380	0.5252	0.0255	0.5924	-0.0393	0.4766	-0.0393	0.7383
	X_5	**-0.0628**	**0.0000**	**-0.0339**	**0.0042**	0.0101	0.5605	-0.0137	0.6867
	X_6	0.0100	0.7334	0.0142	0.4965	0.0667	0.0224	0.0649	0.3598
	X_7	0.0152	0.2217	0.0009	0.9383	-0.0162	0.4514	-0.0062	0.8168
	X_8	0.0520	0.0200	0.0340	0.0654	0.0176	0.5818	0.1078	0.0354
	X_9	-0.2215	0.0186	-0.0334	0.5668	0.0051	0.9116	0.0059	0.9668
	X_{10}	-0.1196	0.6610	-0.1889	0.2409	0.2481	0.1050	0.2727	0.2617
All/Any Distress	X_1	0.0625	0.0006	0.0257	0.0454	0.0216	0.2424	0.0125	0.4582
	X_2	0.1896	0.0039	0.0450	0.3329	-0.0428	0.2327	0.0418	0.4942
	X_3	-0.1582	0.0000	-0.0660	0.0082	0.0594	0.0105	0.0267	0.5042
	X_4	0.0873	0.1055	0.0657	0.1448	-0.0406	0.1501	0.0063	0.8819
	X_5	-0.0575	0.0000	-0.0248	0.0186	0.0136	0.1723	0.0134	0.2599
	X_6	0.0572	0.0351	0.0154	0.4309	-0.0130	0.4872	0.0116	0.6758
	X_7	0.0301	0.0112	0.0149	0.1787	-0.0043	0.6920	-0.0349	0.0006
	X_8	0.0508	0.0134	0.0348	0.0509	0.0009	0.9662	-0.0423	0.0332
	X_9	-0.0975	0.1757	0.0689	0.1969	0.0034	0.8955	0.0532	0.3245
	X_{10}	0.1267	0.6021	0.1148	0.4270	0.0347	0.7288	0.2087	0.0991

0.0625 *Blue text denotes positive relationship*

-0.1038 *Red text denotes negative relationship*

0.0200 *Green text and fill denotes significant correlation at $\alpha = 0.05$*

X_3 *Bold highlighted denotes significant correlation and consistent across multiple datasets*

[a] *Coeff = The coefficient fit to the linear term in the regression by maximum likelihood estimation*

[b] *Sig = p value determined from the likelihood ratio ($\alpha = 0.05$).*

6.2 Shear wave velocity statistical analysis

The predictors applied to the thickness analysis were designed to measure structural and geometric changes. Velocity is based on materials properties, so most of the thickness predictors do not apply. Therefore, average velocity per traverse was analyzed in the regression results.

- Transverse Joint Spalling

As previously stated, traverse joint spalling is a major distress type in all four surveys. The velocity regression results for traverse joint spalling show a weak ($p<0.05$), but significant, negative correlation between velocity and traverse joint spalling for Highway 60 East, Highway 60 West, and Highway 100, as shown in Table 9. Only I-394 does not show this correlation. Investigation of the regression shows that fit models (Figures 19 and 20) only span a narrow range of probabilities, suggesting the model lacks the ability to discriminate distress occurrence from non-occurrence. This weakness, combined with weakness of the correlation suggests that models for transverse joint spalling are not useful.

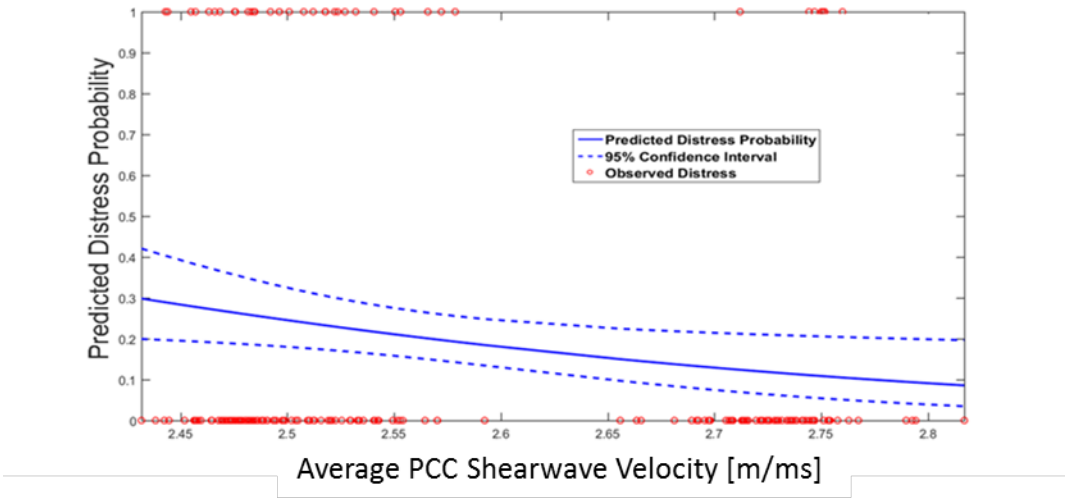

Figure 19 - Highway 60 East (Velocity): Average Traverse Velocity *versus* Transverse Joint Spalling.

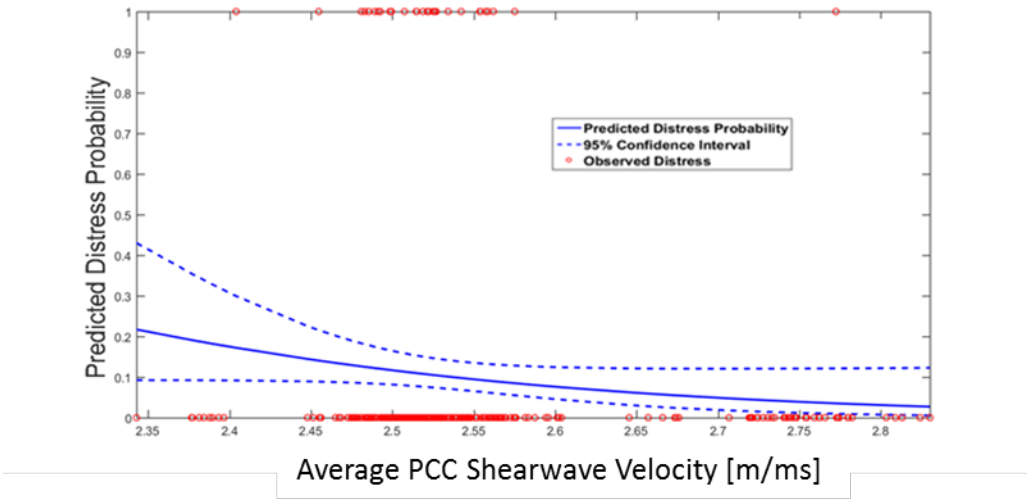

Figure 20 - Highway 60 West (Velocity): Average Traverse Velocity *versus* Transverse Joint Spalling.

- Longitudinal Joint Spalling

Longitudinal joint spalling was only found to be significant only in Highway 100. Therefore, it is concluded that there is no correlation between thickness variability and longitudinal joint spalling

- Cracked and Broken Planes

As with the thickness correlations, Highway 60 East and Highway 60 West datasets are of primary interest when investigating cracked and broken panels. There was a very strong negative correlation ($p < 0.0005$) found between average traverse velocity and cracked and broken panels (Figures 21 and 22 and Table 9). Both of these correlations suggest that pavements with a lower velocity are more likely to exhibit cracked or broken panels.

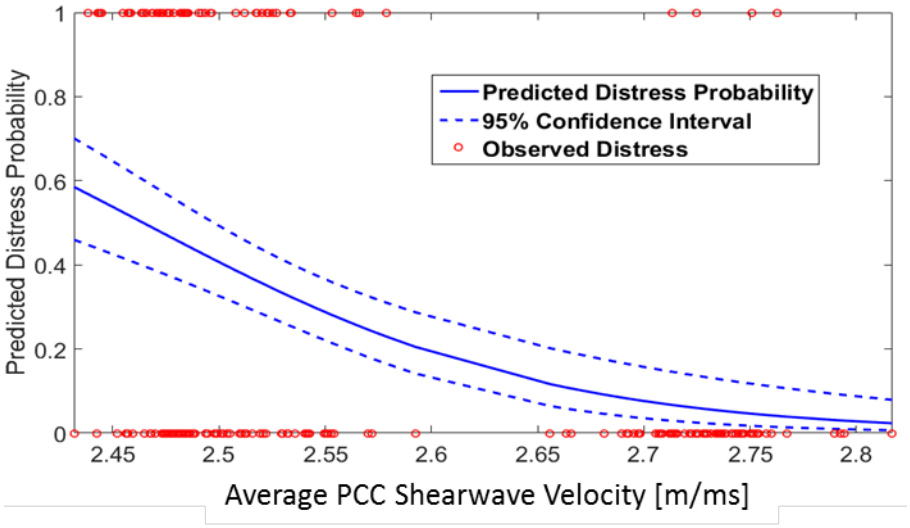

Figure 21 - Highway 60 East (Velocity): Average Traverse Velocity *versus* Cracked and Broken Panel.

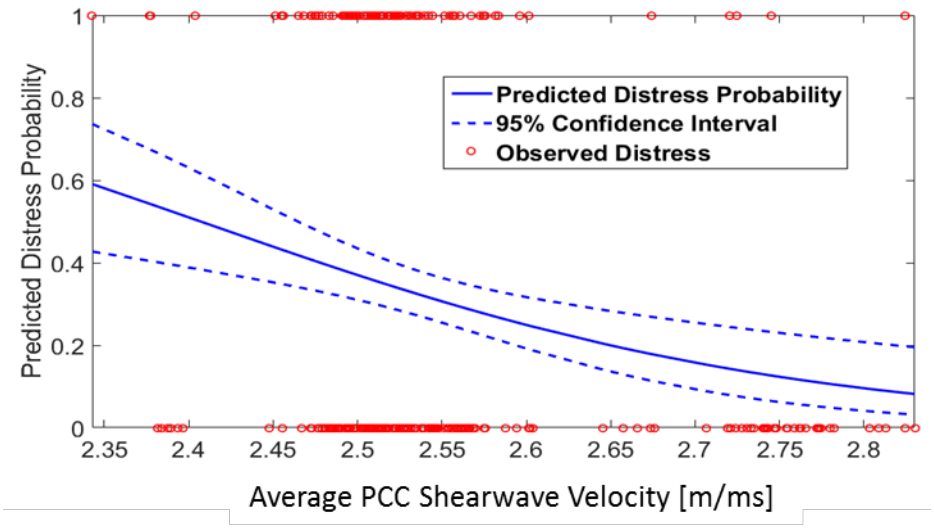

Figure 22 - Highway 60 West (Velocity): Average Traverse Velocity *versus* Cracked and Broken.

- All Distress

A strong negative correlation ($p < 0.005$) was found between average traverse velocity and all distress in all four surveys (Figures 23 to 26, Table 9). This is not particularly surprising for Highway 60 East, Highway 60 West, or Highway 100, as all three were found to have strong significant negative correlations. However, for I-394, all distress is the only strong significant correlation, suggesting the weaker correlations of other distress are all consistent and add to create a highly significant result. The full regression results support this conclusion. Though the other correlations in I-394 are weak, they overwhelming suggest a negative correlation between velocity and distress.

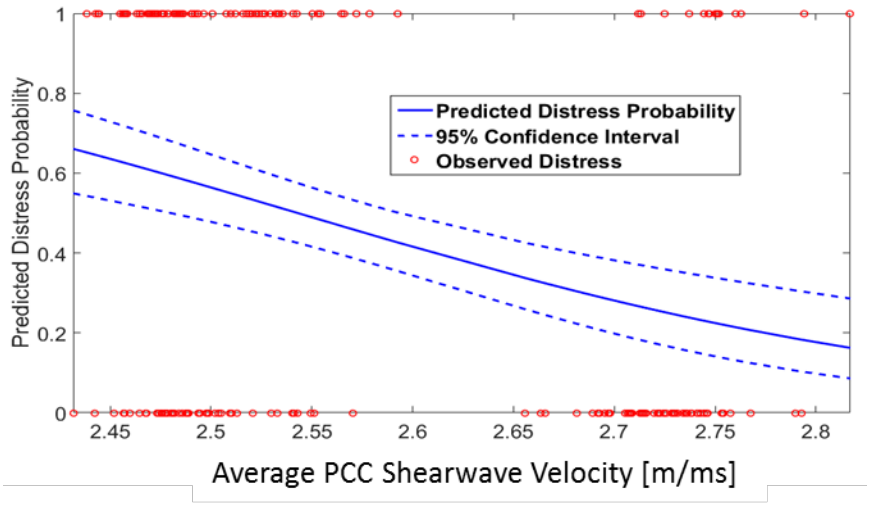

Figure 23 - Highway 60 East (Velocity): Average Traverse Velocity *versus* all Distress.

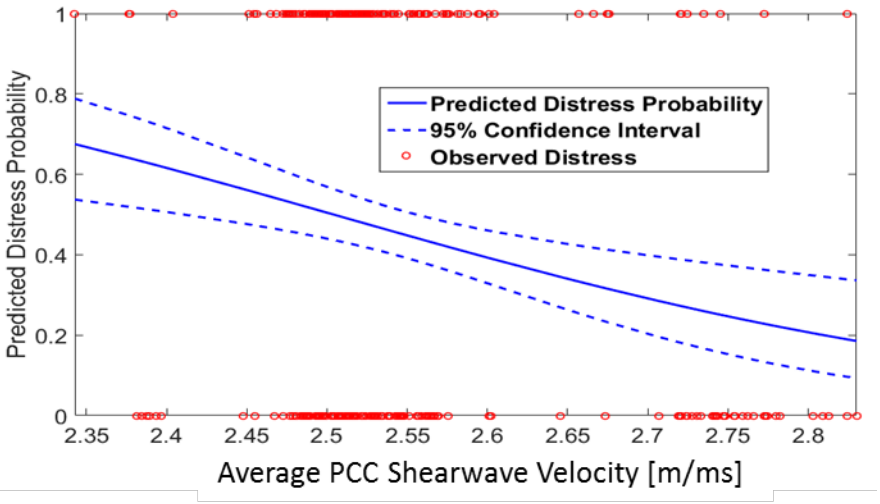

Figure 24 - Highway 60 West (Velocity): Average Traverse Velocity *versus* all Distress.

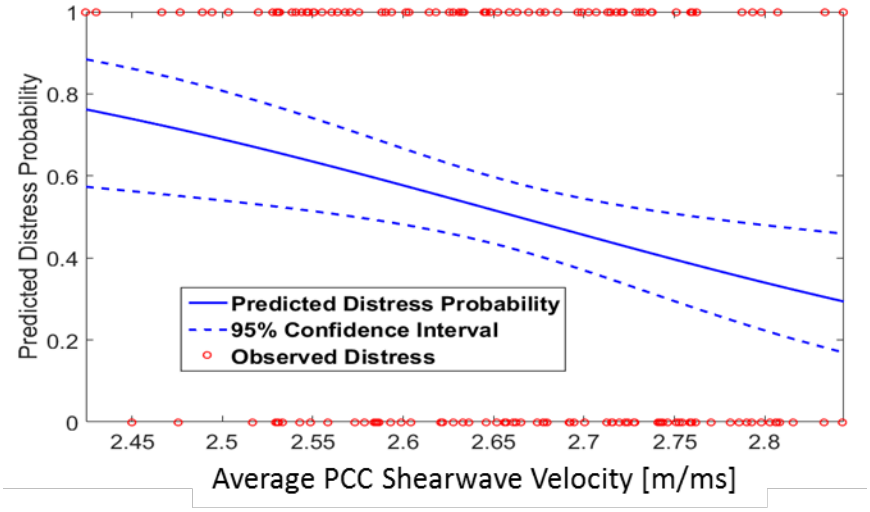

Figure 25 - Highway 100 (Velocity): Average Traverse Velocity *versus* all Distress.

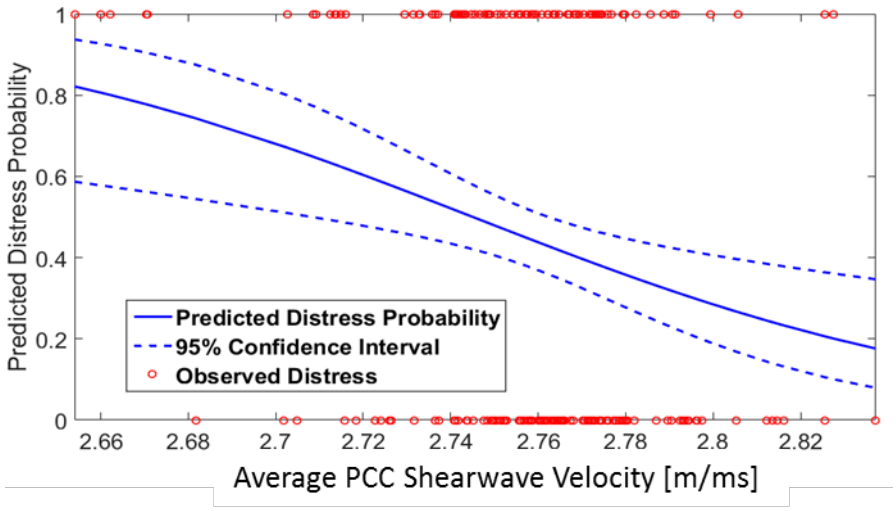

Figure 26 - I-394 (Velocity): Average Traverse Velocity *versus* all Distress.

Table 9 - Average velocity per traverse and distress correlation

	HWY 60E		HWY 60W		HWY 100		I 394	
	Coeff[a]	Sig[b]	Coeff[a]	Sig[b]	Coeff[a]	Sig[b]	Coeff[a]	Sig[b]
Transverse Joint Spalling	**-3.9223**	**0.0162**	**-4.7162**	**0.0472**	**-4.5160**	**0.0463**	-5.3055	0.4203
Longitudinal Joint Spalling	-1.3729	0.4658	-1.5168	0.6159	-8.0306	0.0000	-11.6995	0.0889
Cracked and Broken Panels	**-10.5786**	**0.0000**	**-5.7138**	**0.0001**	0.6179	0.8307	7.2970	0.6018
All/Any Distress	**-5.9865**	**0.0000**	**-4.5366**	**0.0004**	**-6.1279**	**0.0003**	**-16.7573**	**0.0014**

0.0625 *Blue text denotes positive relationship*

-0.1038 *Red text denotes negative relationship*

0.0200 *Green text and fill denotes significant correlation at α = 0.05*

X_1 *Bold highlighted denoted significant correlation and consistent across multiple datasets*

[a] *Coeff = The coefficient fit to the linear term in the regression by maximum likelihood estimation*

[b] *Sig = p value determined from the likelihood ratio (α = 0.05).*

CHAPTER 7: CONCLUSION

A combination of non-destructive ultrasonic thickness tests and distress surveys was performed on three existing Minnesota highways prior to their rehabilitation, in order to investigate possible correlations between Portland cement concrete (PCC) thicknesses and shear wave velocity (SWV) variations with observed surface distresses. Significant variation in measured concrete thickness was observed, but regression analysis of thickness variation and surface distress concludes that exceeding design thickness does not correlate with an increase in pavement performance. High distress concentrations were observed both in areas with deficient and excess thickness. It is important to note that these results do not imply that pavement thickness is irrelevant to performance, or that contractors should not be penalized for thickness deficiencies, as the pavement still needs to have sufficient thickness to carry its intended traffic loadings over it service life.

A more significant and consistent correlation was found with concrete shear wave velocity (SWV). Decreased SWV was found to correlate with increased occurrence of cracked and broken panels as well as the occurrence of any distress type. The thickness and SWV combination analysis examining construction and design data shows that significant correlations generally result from different distress rates associated with changes in pavement construction. Design and construction changes in Highway 60 resulted in segments with different performance as measured by distress concentration. The segments were clearly noticed due to SWV variations. Consequently, it is assumed that an ultrasonic SWV survey is an appropriate test to identify changes in construction and design which may lead to higher rates of distress occurrence.

While the results discussed here are limited by the small number of analyzed sections, they illustrate the importance of material quality and uniformity of control during construction, since alterations in material properties (SWV) may significantly influence pavement performance.

CHAPTER 8: RECOMMENDATIONS FOR SHEAR WAVE VELOCITY TESTING

MIRA Ultrasonic tomography was used to conduct surveys of surface shear wave velocity on several pavements. Two of these surveys were performed on Minnesota State Highway 60 (Highway 60). The surface shear wave velocity surveys conducted on Highway 60 resulted in distinct separations within the data sets. Both datasets contained a high velocity (approximately 2.7 m/ms) and a low velocity section (approximately 2.3 m/ms). Within each velocity section, the velocity was found to have a lower standard deviation than the combined section (Table 10). Variogram (var) analysis was performed and determined that there is no significant spatial correlation of velocity within the individual sections. Sections with lower velocity were correlated with a higher probability of distress occurrence, as seen in Section 3. For Highway 60, the discrepancy in velocity between the two sections was investigated and found to coincide with a change in construction date and concrete mix. The velocity profile of Highway 60E is given in Figure 27. Note two distinct sections are observed. Both sections have similar standard deviation, but different means. A similar profile was observed on Highway 60W as it covers the same segment in an opposite direction.

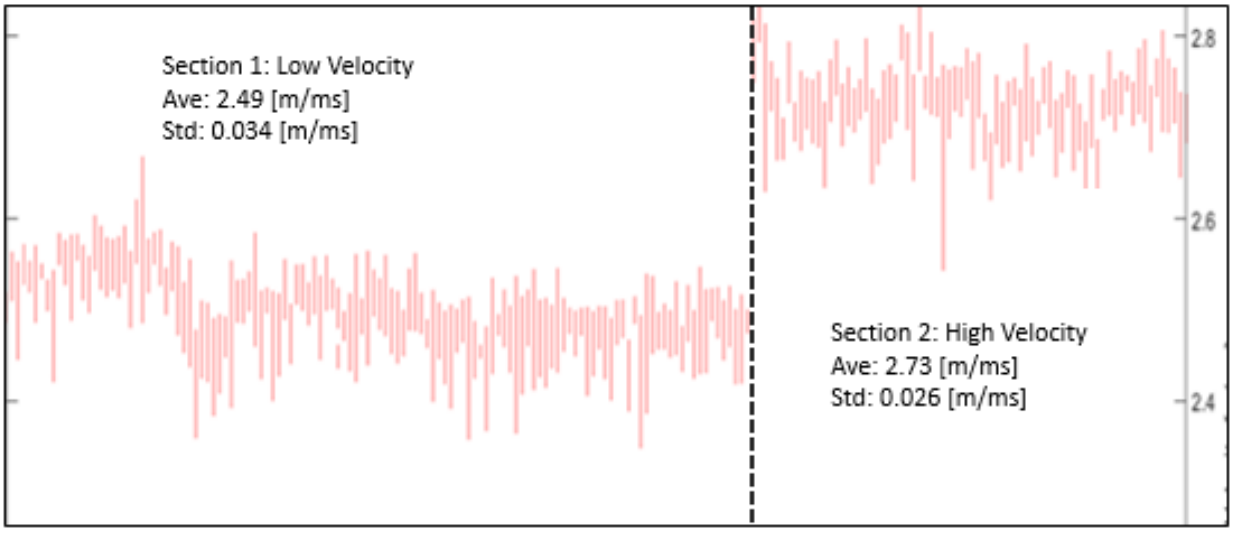

Figure 27 - Surface shear wave velocity profile of Highway 60

Table 10 - Shear wave velocity variability for sections of Highway 60

	Highway 60E			Highway 60W		
Section	Avg. Vel. (m/ms)	Std. dev. (m/ms)	Var. $(m/ms)^2$	Avg. Vel. (m/ms)	Std. dev. (m/ms)	Var. $(m/ms)^2$
High velocity	2.728	0.0261	0.0007	2.754	0.0334	0.0011
Low velocity	2.498	0.0344	0.0012	2.513	0.0447	0.0020
Combined	2.565	0.1099	0.0121	2.547	0.0939	0.0088

The analysis performed above may be applied for the early detections of deficiencies in pavement material properties. As seen in surveys conducted on Highway 60, pavement segments of consistent materials (i.e. when the analysis is performed separately for the segments with high and low velocities) have a standard deviation of shear wave velocity of approximately 0.03 m/ms. If a velocity survey is conducted over a section where material properties change, the standard deviation of the velocity measurements increases dramatically to approximately 0.1 m/ms. Therefore, if a surface shear wave velocity survey is conducted over a section of pavement, a velocity standard deviation greater than a threshold value indicates a potential change in material properties and warrants investigation. Table 10 suggest that 0.1 m/ms can be used as this threshold value until more information is available.

8.1 Surface Shear Wave Velocity Proposed Survey Methodology

1. Surveys must be conducted a minimum of 28 days after concrete was poured to eliminate variation due to degree of curing.

2. Surveys should consider both transverse and longitudinal variation. Therefore a survey pattern of three traverse measurements per slab are suggested. The measurements should be taken half way longitudinally between transverse joints. The traverse locations proposed are as follows (Figure 28):
Location 1: Right Wheel Path
Location 2: Center of Wheel Path
Location 3: Left Wheel Path

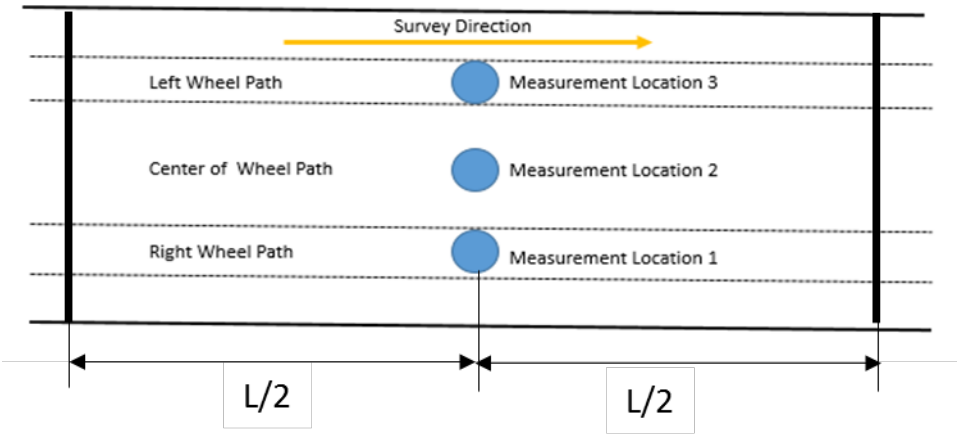

Figure 28 - Shear wave velocity measurement locations per slab.

3. All measurements should be taken in repeated couples. To conduct a repeat measurement, the first measurement is taken, then the MIRA device is lifted and placed in the sample location again, and another measurement is taken. In the final analysis, the couples will be compared to test for error.

4. To produce statically sound results, the survey should be conducted for a minimum of 20 slabs, for a total of 60 couples or 120 total measurements. Such a survey may be expected to take 15-30 min.

5. Special attention should be given to sections which are known to have experienced changes in mix design, construction interruption, or other unusual circumstances.

6. Once data collection is complete, compute the population standard deviation of the shear velocity dataset.

7. If the computed population standard deviation is above 0.1 m/ms, there may be a potential significant change in material properties and further analysis must be completed. If the computed population standard deviation is less than 0.1 m/ms, the section variability is not of concern.

8. If the population standard deviation was found to be greater than 0.1 m/ms, visually plot the velocity data along the survey. If a jump in the surface shear wave velocity can be visually determined, further analysis is required. If no visual jump is apparent, the variability may be due to intrinsic material variability or variation due to the degree of curing, which is not of concern.

9. If a visual jump in the velocity plot is apparent, separate the visually distinct sections and compute the arithmetic mean and standard deviation for each section.

10. Using the mean and standard deviation computed for each section, perform a two-sampled t-test for equal variance. This statistical test will determine if the mean values of the two sections are statistically different. The two-sample t-test for equal variance is given by:

The null hypothesis is given by Equation 22:

$$H_0: \mu_1 - \mu_2 = 0 \tag{22}$$

Whereas, alternative hypothesis is given by Equation 23:

$$H_1: \mu_1 - \mu_2 \neq 0 \tag{23}$$

Where μ_1 is the shear wave velocity mean value of the first section and μ_2 is the mean value of the second section.
The null hypothesis will be rejected at a 95% confidence (Equation 24):

$$\alpha = 1 - 0.95 = 0.05 \tag{24}$$

The statistic can be calculated by Equation 25:

$$t = \frac{(\overline{x_1} - \overline{x_2})}{s_p \left[\left(\frac{1}{n_1}\right)^2 - \left(\frac{1}{n_2}\right)^2\right]} \tag{25}$$

Where t is the computed value for t-statistic; $\overline{x_1}$ is the arithmetic average of the first section; $\overline{x_2}$ is the arithmetic average of the second section; n_1 is the number of measurements within the first section; n_2 is the number of measurements within the second section; and s_p is the pooled variance.

The pooled variance given by Equation 26:

$$s_p = \sqrt{\frac{(n_1 - 1) * {s_1}^2 + (n_2 - 1) * {s_2}^2}{n_1 + n_2 - 2}} \tag{26}$$

Where s_1 is the population standard deviation of section 1 and s_2 is the population standard deviation of section 2.

The degrees of freedom associated with the statistical test are calculated by Equation 27:

$$\delta = n_1 + n_2 - 2 \tag{27}$$

Where δ is the degrees of freedom for the t-test.

The t-statistic can now be used to determine the p-value for the hypothesis test (Equation 28).

$$p - value = \Pr(T \geq t | df = \delta) \tag{28}$$

If the computed $p - value$ is less than the previously defined α, the null hypothesis is rejected and the difference in the pavement sections are determine to be statistically significant. A t-test is easily implemented in Microsoft Excel, MATLAB, and other commonly available analytical applications.

11. If the results of the t-test determined statistical significance for the visual jump, follow up investigation is suggested. Validation of mix design, coring, additional surveying and review of construction records is advised to find explanations on the change in material properties disclosed by the analysis.

- **Future Study**

The surface shear wave velocity surveys performed on Highway 60 produced strong correlations between concrete shear wave velocity and pavement performance and showed that determining shear wave velocity could be a valuable method to identify changes in pavement properties. The protocol outlined above is a direct result of these findings. As a result, the developed procedure is applicable for fairly mature concrete, but cannot be used shortly after concrete placement when some of the variability in the concrete properties may be a result of natural variability in the degree of cement hydration.

Results of a recent MnDOT-sponsored study suggest however that the variation in concrete properties can be adjusted for the concrete age, even for early age concrete. In order to better understand processes resulting in velocity changes and to further refine velocity surveys as a QA/QC method, more data is needed. That could be a subject of a subsequent study.

REFERENCES

An, J., Nam, J., Kwon, S., and Joh, S. (2009). "Estimation of the Compressive Strength of Concrete Using Shear Wave Velocity." *New Technologies in Construction and Rehabilitation of Portland Cement Concrete Pavement and Bridge Deck Pavement*: pp. 154-164.

Cho, M. R., Joh, S. H., Kwon, S. A., and Kang, T. H. (2007). "Nondestructive In-Place Strength Profiling of Concrete Pavements by Resonance Search Technique," *Proc. of 86th Annual Meeting of the Transportation Research Board*, January 21-25, 2007, Washington, D.C.

Edwards, L. (2012). "Evaluation of Technologies for Nondestructively Determining Concrete Pavement Thickness," *Proceedings of the 10th International Conference on Concrete Pavement*, International Society of Concrete Pavements, July 8-12, 2012, Québec City, Canada.

Freeseman, K., Hoegh, K., and Khazanovich, L. (2016a) "Characterization of concrete at various freeze-thaw damage conditions using SH-waves." *AIP Conference Proceedings* 1706, 020017.

Freeseman, K., Hoegh, K., and Khazanovich, L. (2016b). *Concrete Strength Required to Open to Traffic*. Report No. MN/RC 2016-01, Minnesota Department of Transportation. St. Paul, MN.

Heisey, J., I. Stokoe, and A. Meyer (1982). "Moduli of pavement systems from spectral analysis of surface waves." *Transportation Research Record* 852: 22-31.

Hoegh, K., Khazanovich, L., and Yu, H. (2011) Ultrasonic Tomography for Evaluation of Concrete Pavements. *Transportation Research Record* 2232: 85-94.

Hosmer, D. W., Lemeshow, S., and Sturdivant, R. X. (2013).*Wiley Series in Probability and Statistics, Applied Logistic Regression* (3rd Edition). New York, NY, USA: John Wiley & Sons.

Jiang, Y., Selezneva, O., Mladenovic, G., Aref, S., and Darter, M. (2003) Estimation of Pavement Layer Thickness Variability for Reliability-Based Design. *Transportation Research Record* 1849: 156-65.

Kim, S. M., McCullough, B. F. (2002) Reconsideration of Thickness Tolerance for Concrete Pavements Report No. 4382-1, Federal Highway Administration, Washington, DC.

Miller, J. Bellinger, W. Y. (2003) Distress identification manual for the Long-Term Pavement Performance Program, Report No. FHWA-RD-03-031, Federal Highway Administration, Washington, DC.

Minnesota Department of Transportation. (2003). *Mn/DOT Distress Identification Manual*. Minnesota Department of Transportation, St. Paul, MN.

Minnesota Department of Transportation. (2005). *Standard Specifications for Construction*. Minnesota Department of Transportation, St. Paul, MN.

Minnesota Department of Transportation. (2016). Projects on Minnesota highways, updated March 24, 2016. Available: http://www.dot.state.mn.us/roadwork/current.html

Selezneva, O. I., Jiang, Y. J., and Mladenovic, G. (2002) Evaluation and Analysis of LTPP Pavement Later Thickness Data, Report No. FHWA-HRT-12-041, Federal Highway Administration, Washington, DC.

Stubstad, R. N., Tayabji, S. D., Lukanen, E. O. (2002) LTPP Data Analysis: Variations in Pavement Design Inputs, Report No. Project 20-50[5]), National Cooperative Highway

Research Program Transportation Research Board National Research Council, Washington, DC.
Vancura, M. E. (2013) Evaluation of In-Situ Variability of Concrete Pavement Characteristics and Their Effect on Performance. Thesis. University Of Minnesota, Minneapolis, MN.